A review of acoustic measurement of small-scale sediment processes

Peter D. Thorne[a,*], Daniel M. Hanes[b]

[a] *Proudman Oceanographic Laboratory, Bidston Observatory, Prenton, Merseyside CH43 7RA, UK*
[b] *Civil and Coastal Engineering Department, University of Florida, Gainesville, FL 32611, USA*

Abstract

Over the past two decades the application of acoustics to the measurement of small-scale sediment processes has been gaining increasing acceptance within the sedimentological community. This has arisen because acoustics has the potential to measure non-intrusively, with high temporal and spatial resolution, profiles of suspended sediment size and concentration, profiles of flow, and the bedform morphology. In the present article we review the capability of acoustics to deliver on its potentiality to make a valuable and unique contribution to the measurement of small-scale sediment processes. The article introduces the reasons for using acoustics, the physics underlying the approach, a series of examples illustrating collected data, a discussion on some of the difficulties encountered when applying acoustics and finally a look to the future and possible new developments. © 2002 Elsevier Science Ltd. All rights reserved.

1. Introduction

The development of our understanding of small-scale sediment transport processes in the coastal zone has benefited greatly from the recent development of field deployable instruments capable of measuring the significant physical processes. In particular, instruments based on the scattering of underwater sound (Thosteson and Hanes, 1998; Hay and Wilson, 1994; Zedel et al., 1996; Thorne and Hardcastle, 1997), and light (Downing et al.,

1981; Ludwig and Hanes, 1990; Sternberg et al., 1991; Bunt et al., 1999; Agrawal and Pottsmith, 1993, 1994, 2000), have been developed for studying sediment processes under waves and currents. Optical instruments are presently in more common use than acoustics for suspended sediment measurements. However, the potential of acoustics to provide the required parameters for assessing and developing sediment transport formulae is significantly greater, although obviously most studies gain by a synergy of optics, acoustics and conventional instrumentation (Lynch et al., 1994, 1997a; Green et al., 1999).

The measurement of these parameters can conveniently be divided into three components for small-scale studies of sediment transport

*Corresponding author. Tel.: +44-151-653-8633; fax: +44-151-653-6269.

E-mail addresses: pdt@pol.ac.uk (P.D. Thorne), hanes@ufl.edu (D.M. Hanes).

dynamics: (i) the seabed morphology, (ii) the sediment field, and (iii) the hydrodynamics. These three components interrelate with each other in complex ways, being mutually interactive and interdependent as illustrated schematically as a triad in Fig. 1. For example, flow separation and vortex generation due to flow over ripples on the seabed influences the suspension of sediment. Further, the shape of the ripples contributes to the overall flow resistance and the flow structure in the boundary layer. Yet the ripples themselves are a product of the local sediment transport.

A vision of a number of people (Jansen, 1979; Young et al., 1982; Clarke et al., 1984; Schaafsma

and Kinderen, 1985; Hanes and Vincent, 1987; Hanes et al., 1988; Libicki et al., 1989; Lynch et al., 1991; Hay and Sheng, 1992; Crawford and Hay, 1993; Thorne et al., 1993; Thorne and Hardcastle, 1997) involved in studying small-scale sediment processes in the coastal zone over the past two decades, has been to attempt to utilise the potential of acoustics to simultaneously and non-intrusively measure seabed morphology, the suspended sediment particle size and concentration profile, and the velocity profile, with the required resolution to observe the perceived dominant sediment processes. The capabilities to measure the three components have developed at different rates, and it is only in the past few years that the potentiality of an integrated acoustic approach for measuring the triad has become realizable (Thorne et al., 1998a; Traykovski et al., 1999).

The concept of using acoustic diagnostics in the underwater environment is attractive and straightforward as illustrated by the schematic of acoustic application in Fig. 2. A pulse of high frequency sound, typically in the range 0.5–5 MHz in frequency, and centimetric in length, is transmitted from a directional sound source usually mounted a metre or two above the bed, and the backscattered signal gated into range bins and digitised. As the pulse propagates down towards the bed, sediments in suspension
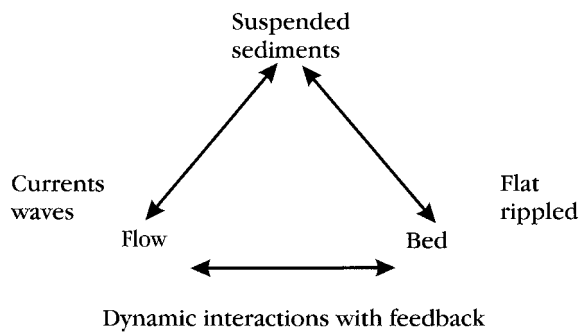
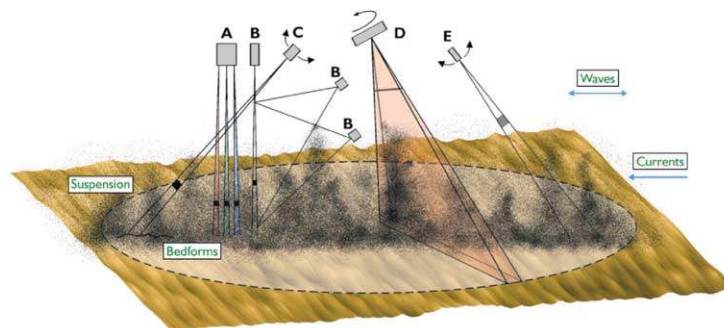Fig. 1. Illustration of the sediment processes triad and their interactions.

Fig. 2. Schematic of the application of acoustics. The figure shows a vision of the application of acoustics to sediment transport processes. A—Multifrequency acoustic backscatter for measuring suspended sediment particle size and concentration profiles. B—Coherent Doppler velocity profiler for measuring the three orthogonal components of flow velocity. C—Bed ripple profiler for measuring the bed morphology along a transect. D—High resolution sector scanner for imaging the local bed features. E—Backscatter scanning system for measuring the relationship between bedform morphology and suspended sediments.

backscatter a proportion of the sound and the bed generally returns a strong echo. The former has the potential to provide information on profiles of suspended sediment parameters and flow, while the latter provides the time history of the bed location. The objective of using acoustics has been to obtain profile measurements of the suspended sediment and flow with sufficient spatial and temporal resolution to allow turbulence and intra-wave processes to be probed, which, coupled with the bedform morphology observations, would provide sedimentologists and coastal engineers with new measuring capabilities to advance our understanding of sediment entrainment and transport.

In the present paper we intend to provide an appraisal of acoustics to deliver the triad of measurements. It is considered by the authors that such a review will be of value at this stage in the development of the subject of sediment-acoustics as an introduction to the field, as a consolidation of the literature on this topic which is spread among acoustic, instrumentation and sediment journals, and to clarify the applications and utilisation of acoustics. The paper is structured as follows: (2) an explanation of the basic physics which is used to interpret the backscatter signal, and (3) a description of how the acoustic systems are calibrated. Some readers may wish to defer reading (2) and (3) until they have read the applications section and decided whether acoustics can contribute to their studies. (4) Illustrations of the use of acoustics in the observation of small-scale sediment processes, both in large-scale flume facilities and in the field. (5) Discussion on the limitations and deployment difficulties of present instrumentation and a forward look to new developments.

Finally, the authors do not want to give the impression that all can and will be done by acoustics. We see it as a complementary tool to optics and more traditional measurement methods. However, the theoretical framework, which underpins the acoustic approach, coupled with its capability to profile non-intrusively and measure the bed, the flow, and suspended sediments simultaneously, makes it a uniquely useful tool for sediment process studies.

2. Acoustic methodology

The present section provides an overview of the background to the theoretical frame work used to interpret backscattered signals from suspensions of non-cohesive sediments, and how to extract sediment and flow parameters and measure the bedform morphology.

2.1. Concentration and particle size

The following approach precis recent works (Sheng and Hay, 1988; Thorne and Campbell, 1992; Hay and Sheng, 1992; Thorne et al., 1993; Crawford and Hay, 1996; Thorne and Hardcastle, 1997) on acoustic backscatter systems, ABS. (Such systems are now commercially available (Smerdon, 1998)). The starting point is the description of the scattered pressure, P_s, from a single particle acoustically insonified. This can be written as

$$P_s = \frac{a_s f P_i}{2r_1} e^{i(\omega t - r_1(k - i\alpha_w))} \tag{1}$$

P_i is the incident pressure on the particle, r_1 is the range from the particle, a_s is the equivalent particle radius, f is known as the form function and describes the scattering properties of the particle, ω and k are respectively the angular frequency and wave number of the sound in water, and α_w is the sound attenuation due to water absorption. The incident pressure on the particle in the farfield of a transducer is given by

$$P_i = \frac{P_0 r_0}{r_2} D e^{i(\omega t - r_2(k - i\alpha_w))} \tag{2}$$

P_0 is the reference pressure normally defined at $r_0 = 1$ m, r_2 is the range from the transducer, and D is the directivity function of the transducer. For backscatter measurements a monostatic configuration is employed, and the same transducer is used for transmission and reception, i.e., in transceiver mode. Substituting Eq. (2) into Eq. (1) and noting the directivity of the transducer on reception gives

$$P = \frac{a_s f P_0 r_0 D^2 e^{i(\omega t - 2r(k - i\alpha_w))}}{2r^2}. \tag{3}$$

Now, if we consider an elemental volume of scatters, δv, the elemental mean-square backscattered signal, δP_{ms}, for incoherent scattering (i.e.,

the backscattered phase is random and uniformly distributed over 2π) can be written as

$$\delta P_{ms} = N \langle PP^* \rangle \delta v. \tag{4}$$

P^* is the complex conjugate of P, $\langle \ \rangle$ represents an ensemble average over a number of backscatter returns, and N is the number of particles per unit volume. To form the root-mean-square, P_{rms}, Eq. (4) needs to be integrated over the volume of insonification. If a circular piston source is used for the transceiver, the integration can be readily expressed in spherical polar coordinates with $\delta v = r^2 \sin\theta \, d\theta \, d\phi \, dr$, this allows P_{rms} to be expressed as

$$P_{rms} = P_0 r_0 \langle f \rangle \left\{ \frac{3M}{16\pi \langle a_s \rangle \rho_s} \right\}^{1/2}$$

$$\left\{ \int_{r-\tau c/4}^{r+\tau c/4} \int_0^{\pi/2} \int_0^{2\pi} \frac{e^{-4\alpha r}}{r^2} D^4(\theta) \sin\theta \, d\phi \, d\theta \, dr \right\}^{1/2}, \tag{5}$$

N has been replaced by the mass concentration $M = (4/3)\pi \langle a_s^3 \rangle \rho_s N$, ρ_s is the density of the particles in suspension, $\langle \ \rangle$ represents an average over the particle size distribution, and $\langle f \rangle = \left\{ \langle a_s \rangle \langle a_s^2 f^2 \rangle / \langle a_s^3 \rangle \right\}^{1/2}$. $\alpha = \alpha_w + \alpha_s$ where α_s is the attenuation due to the sound propagating through the suspension of suspended sediments. τc is the pulse length, where τ is the pulse duration, and c is the velocity of sound in water. If the attenuation over the insonification volume is relatively small (see Hay, 1991 for the correction factor when this assumption is invalid) the exponential term can be moved outside the integral and the integrals can be written as

$$\int_0^{2\pi} d\phi = 2\pi, \tag{6a}$$

$$\int_{r-\tau c/4}^{r+\tau c/4} \frac{1}{r^2} dr = \frac{\tau c}{2r^2}, \quad \tau c \ll r, \tag{6b}$$

$$\int_0^{\pi/2} D^4(\theta) \sin\theta \, d\theta = \left\{ \frac{0.96}{ka_t} \right\}^2, \quad ka_t \geqslant 10, \tag{6c}$$

where $D(\theta) = 2J_1(ka_t \sin\theta)/(ka_t \sin\theta)$ a_t is the transceiver radius, and the details of integrating (6c) have been previously presented (Thorne and

Hardcastle, 1997). Rearranging Eq. (5), using Eq. (6), and expressing in terms of recorded voltage

$$V_{rms} = \frac{k_s k_t}{\psi r} M^{1/2} e^{2r\alpha} \tag{7}$$

$$k_s = \frac{\langle f \rangle}{\sqrt{\langle a_s \rangle \rho_s}} \quad k_t = RT_v P_0 r_0 \left\{ \frac{3\tau c}{16} \right\}^{1/2} \frac{0.96}{ka_t}$$

ψ has been introduced to account for the departure from spherical spreading within the transceiver nearfield (Downing et al., 1995). $V_{rms} = R T_v P_{rms}$ where R is the transducer receive sensitivity, and T_v is the voltage transfer function of the system. For fixed system settings, k_t is a constant or a function of range if time varied gain is applied.

The term which still requires expanding upon is the attenuation α. α_w is relatively straightforward and its dependence upon water temperature, depth and salinity can be obtained from tables or by formulae (Kaye and Laby, 1986. Medwin and Clay, 1998). The sediment attenuation is due to absorption and scattering. For noncohesive sediments insonified at megahertz frequencies the scattering component dominates (Richards et al., 1996). The sediment attenuation can be described by

$$\alpha_s = \frac{1}{r} \int_0^r \xi(r) M(r) dr, \tag{8}$$

where ξ is known as the sediment attenuation constant and is written as

$$\xi = \frac{3}{4\langle a_s \rangle \rho_s} \langle \chi \rangle, \tag{9}$$

$\langle \chi \rangle = \langle a_s \rangle \langle a_s^2 \chi \rangle / \langle a_s^3 \rangle$ and χ is the normalised total scattering cross-section.

It therefore only remains to specify the backscattering and attenuating characteristics of the sediment to evaluate Eq. (7). Fig. 3 shows measurements of f and χ for suspensions of sediments and individual irregularly shaped particles from a number of sources. The data show a general trend with a degree of scatter. The variation in scattering is associated with the detailed particle shape (the composition of the particles in the figures was primarily quartz) as shown by Schaafsma and Hay (1997). The form of the data can be represented by
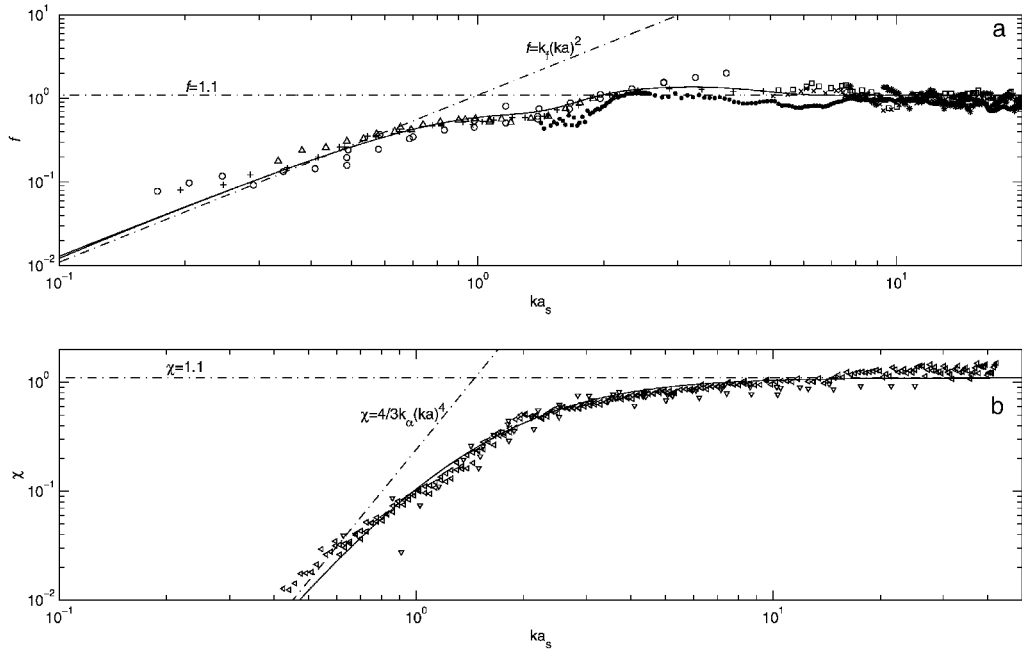
Fig. 3. (a) Measurements of the form function, and (b) the normalised total scattering cross-section. ▽ Sheng and Hay, 1988; + Hay, 1991; △ Cheng and Hay, 1993; ● Thorne et al., 1995a; ◁ Schaafsma, 1995–1998; □ × Thorne et al., 1997; ○ Thorne and Butler, 2001. The solid lines are given by Eq. (10a) and (10b).

relatively simple expressions (Sheng and Hay, 1988, Crawford and Hay, 1993; Thorne et al., 1993).

$$f = C_0 \left\{ \frac{k_f x^2}{1 + k_f x^2} \right\}, \tag{10a}$$

$$C_0 = 1.1\{1 - 0.25 \exp[-((x - 1.4)/0.5)^2]\}$$

$$\{1 + 0.37 \exp[-((x - 2.8)/2.2)^2]\},$$

$$\chi = \frac{1.1(4/3)k_\alpha x^4}{[1 + 1.3x^2 + (4/3)k_\alpha x^4]}, \tag{10b}$$

where $k_f \approx 1.1$, $k_\alpha \approx 0.18$ and $x = ka_s$.

2.2. Statistics

Eq. (7) provides an expression for the root-mean-square voltage. The solution is formulated in terms of a statistical mean because individual realisations of the backscattered signal from a homogeneous suspension of fixed concentration is not constant, but variable due to the random phase of the returns from the scatterers. A single profile provides no useful information on the suspension. The outcome of random phase statistics uniformly distributed over 2π results in a probability distribution for the backscatter signal, V, which is Rayleigh (Thorne et al., 1993) and given by

$$p(V) = \frac{2V}{V_{ms}} e^{-\{V^2/V_{ms}\}}, \tag{11a}$$

where V_{ms} is the mean-square voltage. The standard error in V_{rms} can be expressed as

$$\sigma_e(V) = \left\{ \frac{4 - \pi}{4n} \right\}^{1/2} V_{rms}, \tag{11b}$$

which can be approximated as

$$\sigma_e(V) \approx \frac{V_{rms}}{2\sqrt{n}}, \tag{11c}$$

where n is the number of independent profiles averaged to form V_{rms}. It can be seen that to obtain 5% accuracy in V_{rms} requires approximately 100 independent measurements of V; this will nominally equate to a 10% precision in M. The importance of the statistical nature of the backscatter signal is that there may need to be a degree of compromise between the spatial (i.e. range bin averaging) and temporal resolution (i.e. temporal averaging) and the required accuracy for M.

The above effectively completes the forward problem, i.e., if we know all the parameters we can predict V_{rms} and compare with observations. This comparison has been carried out (Hay, 1991; Thorne and Campbell, 1992; Thorne et al., 1993) and Eq. (7) accurately predicts the backscatter signal from suspensions. The problem of interest to sedimentologists is the capability of ABS used in an inverse mode to extract suspension parameters from the backscattered signal.

2.3. Inverse problem

Rearranging Eq. (7) we have for the suspended sediment concentration

$$M = \left\{ \frac{V_{rms}\psi r}{k_s k_t} \right\}^2 e^{4r\alpha}. \tag{12}$$

Assuming the system has been calibrated, i.e., k_t is known, k_s and α_s are required to evaluate Eq. (12). To evaluate k_s and α_s requires a knowledge of $\langle a_s \rangle$ and M with range from the transducer, and therein lies the problem, these parameters are the ones we are trying to extract from the acoustic signal and are unknown.

2.3.1. Implicit iterative approach

If only a single frequency is available, some estimate is used for $\langle a_s \rangle$, usually based on the local bed sediments, this allows k_s and ξ to be calculated. If the assumption can be made that $\alpha_s \approx 0$, due to $M\xi \ll 1$, then

$$M_0 = \left\{ \frac{V_{rms}\psi r}{k_s k_t} \right\}^2 e^{4r\alpha_w} \tag{13}$$

All the terms on the RHS of Eq. (13) are therefore known or estimated, and the concentration profile

M_0 can be readily evaluated. If it cannot reasonably be assumed that $\alpha_s \approx 0$, an iterative approach is used. Firstly, $\alpha_s = 0$ is used and Eq. (13) evaluated to obtain M_0. M_1 is then estimated using $M_1 = M_0 e^{4r\alpha_s}$, where α_s is calculated using the M_0 profile. This iterative process is repeated until M_n and M_{n+1} are convergent. This approach has been previously considered (Thorne et al., 1993; Thorne and Hardcastle, 1997) and caution needs to be applied with the implicit iterative approach because the iterative feedback between M and α_s is positive and can lead to the solution diverging to zero or infinity due to increasing feedback errors as the solution is propagated from the transducer down to the bed.

If multiple frequencies are available $\langle a_s \rangle$ need not be assumed and M and $\langle a_s \rangle$ can be obtained acoustically. Typically to date three frequencies have been used, normally in the range 1–5 MHz. Rearranging Eq. (12) we can write (Hay and Sheng, 1992).

$$\frac{\langle f_i \rangle}{\langle f_j \rangle} = \frac{(\psi_i V_{rmsi}/k_{ti})}{(\psi_j V_{rmsj}/k_{tj})} e^{2r(\alpha_i - \alpha_j)}, \tag{14a}$$

$$M_i = \left\{ \frac{V_{rmsi}}{k_{si} k_{ti}} \right\}^2 \psi_i^2 r^2 e^{4r\alpha_i}, \tag{14b}$$

where $i \neq j$ and i and j refer to the three frequencies. If, as with the single frequency case, $\alpha_i \approx 0$ and $\alpha_j \approx 0$ is a reasonable assumption, the implicit iterative solution need not be applied. If this is the case $\langle a_s \rangle$ can be extracted from the form function ratio at the different frequencies. In general the suspended sediments will have a size distribution, and therefore $\langle f \rangle$ is obtained from f using an estimated probability distribution for a_s; this effectively acts as a smoothing function on f. Further, as described in Thorne and Hardcastle (1997) estimating $\langle a_s \rangle$ from $\langle f_i \rangle / \langle f_j \rangle$ can lead to multiple values of $\langle a_s \rangle$, which can normally be resolved using the three ratios of $\langle f_i \rangle / \langle f_j \rangle$ available from a three frequency system. Also, the range of $\langle f_i \rangle / \langle f_j \rangle$ over which $\langle a_s \rangle$ can be measured is limited. If $k\langle a_s \rangle \ll 1$, inspection of Eq. (10a) shows $\langle f_i \rangle / \langle f_j \rangle = k_i/k_j$, the ratio of the wave number, therefore there is no size information. Similarly, if $k\langle a_s \rangle \gg 1$, $\langle f_i \rangle / \langle f_j \rangle = 1$

and again there is no size information in the form function ratios.

If sediment attenuation cannot be neglected, the implicit iterative approach can be used. Eq. (14a) is evaluated for the first range bin from the transceiver, $\langle a_{s0} \rangle$ estimated, k_{s0} calculated, and M_0 obtained using Eq. (14b). Eq. (14) is then iterated until $\langle a_{sn} \rangle$ and $\langle a_{s(n+1)} \rangle$, and M_n and M_{n+1} converge. This computation is carried out for each range bin and propagated along the backscattered profile to obtain profiles of $\langle a_s \rangle$ and M. As with the single frequency case, there is positive feedback in the inversion, and the limitations on $\langle f_i \rangle / \langle f_j \rangle$ described in the paragraph above apply.

The implicit iterative approach does have its difficulties, however, with careful choice of frequencies and cautious data analysis and processing, accurate profiles of $\langle a_s \rangle$ and M can be obtained and all the advantages provided by acoustics utilised.

2.3.2. Explicit approach

A complementary approach to the ABS implicit inversion method is the explicit approach developed by Lee and Hanes (1995) and further considered by Holdaway and Thorne (1997) and Thosteson and Hanes (1998). The starting point is to take the natural logarithm of Eq. (12)

$$\ln M = 2 \ln V_{rms} + 2 \ln r + 2 \ln \psi - 2 \ln k_s$$
$$- 2 \ln k_t + 4 r \alpha_w + 4 \int_0^r \xi M \, dr. \qquad (15)$$

Utilising

$$\frac{d}{dr} \ln\{F(r)\} = \frac{F'(r)}{F(r)},$$

where the prime denotes differentiation wrt to r, we can write

$$M' - 2 \left\{ \frac{V'_{rms}}{V_{rms}} + \frac{1}{r} + \frac{\psi'}{\psi} - \frac{k'_s}{k_s} + 2\alpha_w \right\} M = 4 \xi M^2. \qquad (16)$$

In deriving Eq. (16) the assumption has been made that k_t is independent of range, therefore if time varied gain is used in the system this has to have been accounted for in forming V_{rms}. Eq. (16) is a non-linear differential equation of the Bernoulli

type which can be linearised with the substitution $z = M^{1-n}$, where n is the power to which M is raised on the RHS of Eq. (16).

Applying this gives

$$z' + \gamma z = -4\xi, \qquad (17)$$

$$\gamma = 2 \left\{ \frac{V'_{rms}}{V_{rms}} + \frac{1}{r} + \frac{\psi'}{\psi} - \frac{k'_s}{k_s} \right\} + 4\alpha_w,$$

Eq. (17) can be solved using the standard integrating factor method (Weltner et al., 1986) to obtain

$$z e^{\int \gamma dr} = -4 \int \xi e^{\int \gamma dr} + c \qquad (18)$$

γ is readily integrated and results in

$$z\beta^2 = -4 \int \beta^2 \xi \, dr + c, \qquad (19)$$

where $\beta = V_{rms} r \psi k_s^{-1} e^{2\alpha_w r}$. If M and k_s are known at a reference range r_r, and we replace z by M^{-1}, we have

$$M = \frac{\beta^2}{\beta_r^2 / M_r - 4 \int_{r_r}^r \beta^2 \xi \, dr}, \qquad (20)$$

where $\beta_r = \beta$ at $r = r_r$. Eq. (20) has the principle advantage that it does not contain k_t, i.e., there is no requirement to obtain an absolute acoustic and electronic calibration for the system. However, a relative electronic calibration is generally still required to assess the linearity of the system response. Eq. (20) has the disadvantage that some apriori reference information is required to obtain β_r and M_r, and the k_s and ξ (which effectively means $\langle a_s \rangle$) profiles are required to evaluate Eq. (20). Also there is no equivalent expression to Eq. (20) for $\langle a \rangle$ at present, although if multiple frequencies are available the methodology of Thosteson and Hanes, 1998 which combines the implicit and explicit approach can be utilised. However, if only a single frequency is available and we can make the assumption that $\langle a_s \rangle$ is constant with height above the bed and the data analysed is in the transducer farfield, we have

$$M = \frac{\beta_0^2}{\beta_{0r}^2 / M_r - 4\xi \int_{r_r}^r \beta_0 \, dr}, \qquad (21)$$

where $\beta_0 = V_{rms} r e^{2r\alpha_w}$. Eq. (21) provides a simple expression for obtaining M, however, it does have the restriction that $\langle a_s \rangle$ must be constant, and its

value known to evaluate ξ. If it were invalid to use a constant $\langle a_s \rangle$, there is the possibility that the form for the variation of $\langle a_s \rangle$ with range from the transducer could be estimated from a sediment model, or sediment samples collected at a number of ranges, could be used in the evaluation of Eq. (20). If $\langle a_s \rangle$ is constant or its variation with range estimated, the explicit approach still has the limitation that to invert an acoustic profile requires an independent measurement of the suspension. However, this can be circumvented; if M is obtained from Eq. (20), Eq. (12) can be rearranged to give

$$k_t = \beta M^{-1/2} e^{2r\alpha_s}. \tag{22}$$

With k_t now known from the explicit solution, based on independent measurements of the suspension, the implicit approach can be adopted and concentration and particle size profiles calculated independent of reference measurements.

2.4. Flow

To fully utilise the suspension parameters extracted from the backscattered signal, similar hydrodynamic profiles are required. Ideally, if the backscattered signal could be employed for measuring the flow, collocated mass and velocity, and hence sediment flux could be measured directly acoustically. The present section considers the two evolving techniques of coherent Doppler (Lhermitte and Lemmin, 1994; Hardcastle, 1995; Zedel et al., 1996; Lemmin and Rolland, 1997; Hurther and Lemmin, 1998; Zedel and Hay, 1999) and cross-correlation (Thorne et al., 1998b; van Unen et al., 1998; Thorne and Taylor, 2000) to acoustically measure profiles of nearbed flow dynamics. The coherent Doppler is based upon pulse-to-pulse phase coherence between consecutive transmissions to measure the radial component of the velocity along the beam axis. The correlation approach employs a pair of horizontally separated transducers directed vertically downward and cross-correlation of the backscattered signals from the transducer pair is used to obtain flow velocity.

The coherent Doppler velocity profiler, CDVP, uses Doppler shift to obtain the Doppler flow

velocity v_d. For the condition $v_d \ll c$, where c is the sound velocity in water, v_d is given by

$$v_d = \frac{c f_d}{2 f_0} \tag{23}$$

f_d is the Doppler frequency and f_0 is the transmit frequency. To obtain f_d pulse-to-pulse coherence is used and f_d can be expressed as

$$f_d = \frac{1}{2\pi\tau} \tan^{-1} \left\{ \frac{\langle I(t)R(t+\tau) - R(t)I(t+\tau) \rangle}{\langle R(t)R(t+\tau) + I(t)I(t+\tau) \rangle} \right\}, \tag{24}$$

where $R(t)$ and $I(t)$ are the in-phase and quadrature components of the backscattered signal, τ is the time between transmissions and $\langle \rangle$ represents an average over a number of pulse pairs. To obtain unambiguous range velocity measurements we need to have $\tau \leqslant 2r_m/c$ where r_m is the maximum operating range. The maximum unaliased Doppler frequency is given by $f_d \leqslant 1/2\tau$ and therefore we can write the standard range velocity ambiguity equation as

$$r_m v_{dm} \leqslant \frac{c^2}{8 f_0}, \tag{25}$$

where v_{dm} is the maximum unaliased velocity. This sets a limit on the operating range and velocity, although if the velocity direction is known the phase can be unwrapped and the velocities de-aliased.

Unlike the coherent Doppler approach that uses the phase coherence between successive transmissions, the cross-correlation velocity profiler, CCVP, utilises the temporal coherence in the suspension field as it advects beneath two closely spaced transceivers. The backscattered signal from each range bin of the transceiver pair is cross-correlated, the time lag for the suspension to advect from one transceiver to the other obtained, and the velocity profile calculated. The cross-correlation velocity is given by

$$v_c = \frac{d_{12}}{v^*}, \tag{26}$$

where d_{12} is the transducer pair separation and v^* is the time lag at which the normalised cross-correlation reaches its maximum value

$$\rho_{12}(v^*) = \max(\rho_{12}(v)), \tag{27}$$

where

$$\rho_{12}(v) = \frac{R_{12}(v)}{(R_{11}(0)R_{12}(0))^{1/2}} \qquad (28)$$

and $R_{12}(v)$ is the cross-correlation function of the zero mean backscattered ensemble average square voltages from the transducer pair, $v_i^2 = V_{rms_i}^2 - \langle V_{rms_i} \rangle$, $\langle \ \rangle$ represents the average over the record to be cross-correlated and $i = 1$ or 2. R_{12} is given by

$$R_{12}(v) = \int_{-\infty}^{\infty} v_1^2(t,r)v_2^2(t+v,r)\mathrm{d}t, \qquad (29)$$

where v is the lag, r the distance to the range bin, and t is time. Unlike the coherent Doppler system that requires phase coherence between consecutive transmissions, the correlation approach is incoherent, as it is the signal intensity that is used. The basic requirement is that there are fluctuations in the suspension field, which have spatial scales greater than d_{12}, and that these fluctuations can be cross-correlated.

2.5. Bedform morphology

In recent years a number of bed ripple profilers (Vincent and Osborne, 1993; Greenwood et al., 1993; Jette and Hanes, 1997; Bell et al., 1998) and ripple scanners (Hay and Wilson, 1994; Gallagher et al., 1998; Traykovski et al., 1999; Williams et al, 2000) have been developed to measure the local bed morphology. The ripple profilers typically use pencil beam transducers and either via translation, rotation, or using a multiple transducer array measure a transect profile along the bed and its variation over time. The bed location is usually detected using threshold techniques, or as has been done more recently (Bell and Thorne, 1997) the bed echo modelled and this signal cross-correlated with the bed echo.

$$R_{em}(v) = \int_{-\infty}^{\infty} E_e(t)E_m(t+v)\mathrm{d}t, \qquad (30)$$

where e and m refer to the measured and modelled nearbed time-series echo, $E(t)$. The lag, v, at which the maximum value of $R_{em}(v)$ occurs is measured and this is used to locate the bed. This approach has been found to be more robust at tracking the bed location than using simple threshold detection. The ripple profilers provide quantitative measurements along a profile from which parameters such as ripple wavelength and height can be extracted.

The high frequency ripple scanners utilise a fan beam transducer, and provide an image of the bed typically of the order of $10–30\,\mathrm{m}^2$. The images generated are a function of the backscattered signal amplitude from the bed and show areas of high and low return. It is generally not possible from ripple scanners to extract ripple height, however, analysis of the image can yield ripple wavelength, and it importantly provides coverage over an area which present ripple profilers do not.

3. Calibration

To employ the theoretical framework of the previous section to obtain sedimentological measurements from acoustics systems requires calibration. This is particularly the case for the extraction of suspension parameters from the backscattered signal. For the evaluation of Eq. (12) there is the requirement to know k_t, the form of which is given in Eq. (7). There are a number of ways of obtaining k_t, or methods to circumvent the necessity to measure it, and these are discussed below.

One method is a full electronic and acoustic calibration of the system (Thorne et al., 1993; Thorne and Hardcastle, 1997). The electronic calibration requires measuring the transfer function of the system T_v. This includes measuring transmit signal levels, receiving amplification, the form of the time varying gain if any is applied, and the analog to digital conversion. The acoustic calibration requires measurements of the source level, $P_0 r_0$, (Pascal at 1 m), and the receive sensitivity, R, (volts per Pascal), of the transducer. Also to establish a_t generally requires the transducer beam pattern to be measured. For some of the calibration, particularly the acoustic component, specialist equipment is required, and this will not generally be available in most sedimentological laboratories. Also the acoustic calibration is relatively lengthy and requires some background

knowledge in acoustics. Therefore, alternative methods of calibration have been sought.

One alternative approach is to rearrange Eq. (12) and have k_t on the LHS of the equation

$$k_t = \frac{V_{\mathrm{rms}}\psi r e^{2r\alpha}}{k_s M^{1/2}}. \tag{31}$$

Measurements can be conducted on a homogeneous suspension with known scattering characteristics, at a known concentration level, in the farfield of the transducer. Hence k_s, M, and ξ are known and $\psi = 1$. Glass spheres (Hay, 1991) are normally used for the suspension since they are readily available in the required size range, and the scattering characteristics of spheres can be accurately predicted (Thorne et al., 1992). If the electronic gain of the system is constant then k_t has a single value; if time varying gain is applied to the system k_t will be a function of range.

A third approach similar to the above is to conduct measurements on a suspension of sediments and use Eqs. (10a) and (10b) to obtain k_s and ξ. However, the scattering properties of sediments cannot be predicted with the same precision as spheres, and therefore the results for k_t will be less reliable. Alternatively calibration of the acoustic system can be conducted with identical sediments to those found at the field site. The assumption has then to be made that k_s and ξ are invariant in time and height above the bed and therefore $k'_t = k_s k_t$, where

$$k'_t = \frac{V_{\mathrm{rms}}\psi r}{M^{1/2}} e^{2r\alpha} \tag{32}$$

k'_t can then be used to obtain M. This obviously has the limitation that any variations in k_s and ξ will effect the estimate of M, but has the advantage of being simple and does not require k_s to be known.

A further calibration technique is to obtain samples of the suspended sediments in the field contemporaneous and collocated with the acoustic data (Thorne et al., 1998a). If measurements are available at a number of ranges from the transducer, the particle size profile can be estimated, M obtained from Eq. (20) and input into Eq. (31) to obtain k_t. If samples are only available at a single range, Eq. (21) replaces Eq. (20) along

with the caveats associated with Eq. (21). If only a selection of samples are used to obtain k_t, the remainder can be employed to assess the accuracy of the acoustic to sediment parameter inversion algorithm employed. Finally, whichever calibration or inversion technique is used, the stage of development of the application of acoustics to the measurement of suspension parameters is such that in-situ sampling of the suspended sediments can make a valuable contribution to both interpreting and assessing the acoustic measurements.

The above has focused on the calibration of acoustic backscatter systems for measuring suspension parameters. The calibration of the cross-correlation and coherent Doppler velocity measurements is relatively conventional. Normally a flume is used which propagates waves and/or currents seeded with particles which are either entrained from a mobile bed or injected into the water (van Unen et al., 1998). The velocity output from the coherent Doppler or cross-correlation system is then straightforwardly compared with a reference instrument. Effectively it is not a calibration in the ABS sense, since both instruments generate absolute velocities; it is an evaluation of their accuracy, resolution, and dynamic range. Similarly with the scanning systems used to measure the bed microtopograph. The aim is to establish the capability of the system rather than calibrate the instrument. This is usually conducted using a surface with known morphology and comparing the acoustic morphological measurements with the actual (Greenwood et al., 1993).

4. Applications

This is where we hope to convince the reader that the gains of using acoustics outweighs the effort of becoming familiar with employing this technique.

4.1. Suspended sediments

In this section we examine the capability of acoustics to measure suspended sediment concentration and particle size profiles. We do this using a series of illustrations from laboratory calibration

towers, through to large-scale flume facilities and data collected in the marine environment.

4.1.1. Laboratory calibration

As mentioned in the 'Calibration' section, one of the more common methods of calibrating and evaluating an ABS system is to propagate sound through a homogenous suspension of known scatterers and use Eq. (31) to obtain k_t. Fig. 4a shows an example of a sediment calibration tower in use (Thorne and Butler, 2001). The system is recirculating, with water extracted at the base of the tower, re-injected at the top through a mixing unit and further turbulent mixing induced by impellers below the main measurement region. Typically when such towers are filled the water contains a significant concentration of microbubbles and therefore a period, which may be from hours to days, with the system running, is required to reduce background backscatter signal levels to those comparable with the electronic noise of the system. Further low pulse repetition frequencies, typically of the order of a few hertz, are required to allow the sound from one transmission to be dissipated before the following transmission. Sediment is then injected and typically a number of hours are allowed to elapse for the tower to come to equilibrium. Backscatter measurements are then collected on a suspension of known scatterers. A typical example of the results which can be obtained is shown in Fig. 4b. The data in the figure were collected using a suspension of glass spheres of radius 98, 115, 137 and 195 μm using a triple frequency backscatter system operating at 1, 2, and 4 MHz. Fig. 4b show profiles of k_t averaged over the four particle size measurements. If no time varying gain is present or it has been accounted for, then k_t should be constant with range and invariant with the size of the scatterer. This is generally what is seen in Fig. 4, though there is almost always some degree of variability owing to the Rayleigh distribution of the backscatter signal and variability in the homogeneity of the suspension. The results from such measurements provide an absolute calibration for the system that can be used in the acoustic inversion.

4.1.2. Large scale flume facility measurements

Measurements of suspended sediment concentration, wave height, near bed flow velocities and bedform morphology were made in the SISTEX99 (Small-scale International Sediment Transport Experiment) experiment. The goal of SISTEX99 was to simultaneously measure hydrodynamics, sediment dynamics, and bedform morphology at nearly full scale under unidirectional waves. The SISTEX99 experiments were conducted in the Grosser Wellenkanal (Hanover, Germany) wave tank, with dimensions of 300 m in length, 7.5 m deep and 5 m in width, over a 3-month period in the summer of 1999. The test section consisted of a $45 \times 5 \times 0.7\,m^3$ medium sand size bed located at a position 85–130 m from the wave paddle.

The use of acoustic instrumentation combined with the ability to generate specific wave conditions allowed the processes of sand re-suspension over sand beds of well-known characteristics to be examined in considerable detail. Regular (monochromatic), group and random waves were run repeatedly. Suspended sediment profiles were measured with multiple frequency ABS, near bed velocities with acoustic Doppler velocity meters (ADV's), and bedform morphology with an acoustic ripple profiler (MTA, see section 4.3.1). One of the results of these observations is a description of the suspension of sand above a rippled bed under hydrodynamic forcing due to wave groups. This information is useful for examining the effects of time history on the suspension of sand. For example, the measurements can be ensemble averaged over the wave groups to reduce the random fluctuations that appear in any individual realisation. Such an ensemble average is shown in Fig. 5, which show; (a) suspended sand concentration as a function of time and elevation above the seabed, (b) the time series of the flow near the bed, (c) vertical profiles of suspended sediment concentration averaged over each wave in the group and (d) wave-average concentration time series at various elevations above the seabed. It is clear that there exists a time scale for the build up of suspended sediment during the beginning of the wave group and the decay of suspended sediment at the end of the wave group (Vincent et al., 2001). It is anticipated
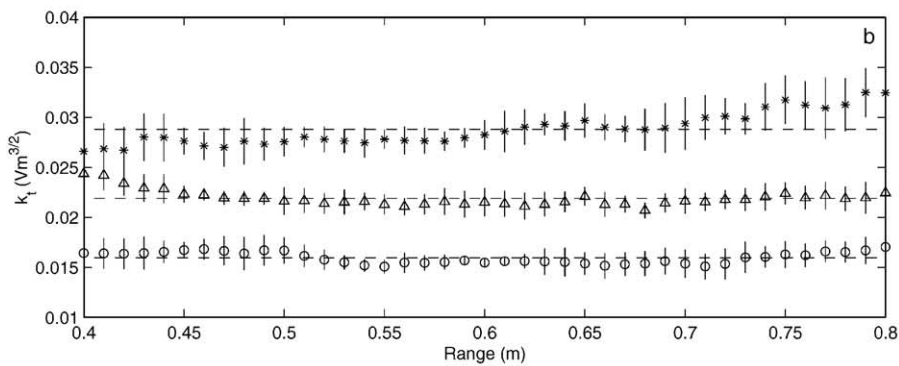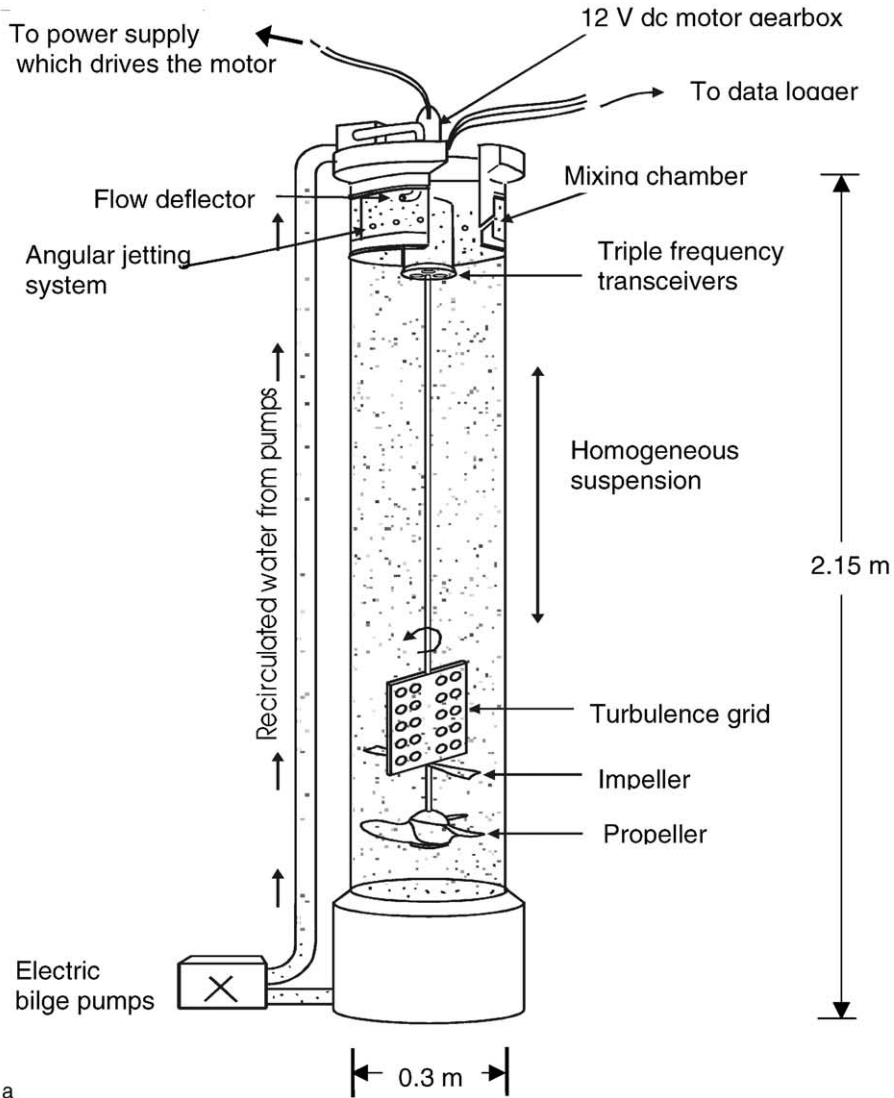
Fig. 4. (a) An example of a suspension tower used to calibrate an acoustic backscatter system, and (b) measurements of k_t obtained for a triple frequency backscatter system operating at o-1 MHz, *−2 MHz, and △ −4 MHz.
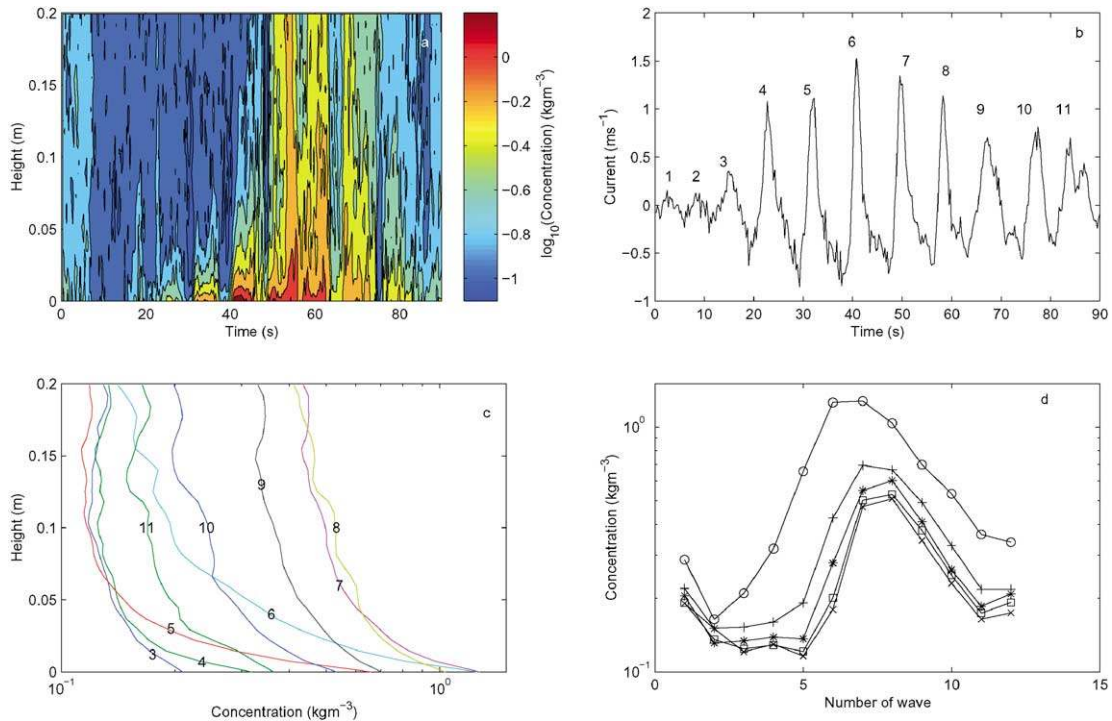
Fig. 5. (a) The temporal and spatial structure of suspended sediments due to a wave group: (b) The along flume flow during the wave group with the wave sequence indicated: (c) the vertical profile of suspended sediment concentration during each wave in the sequence with waves 3–11 shown: (d) The suspended sediment concentration during each wave in the sequence at different elevations above the bed; 0.01 ($\bigcirc$), 0.04 (+), 0.08 (*), 0.12 ($\square$) and 0.16 ($\times$) m.

that the application of acoustics for the examination of the effects of time history during unsteady wave forcing will lead to improved models for sediment transport under realistic wave conditions.

4.1.3. Measurements in the marine environment

A number of publications on the marine deployment of the ABS have now been reported. These include Vincent and Green, 1990; Hanes, 1991; Vincent et al., 1991; Thorne et al., 1993; Hay and Sheng, 1992; Hay and Bowen, 1994; Sheng and Hay, 1995; Osbourne and Vincent, 1996; Lee and Hanes, 1996; Lynch et al., 1997a, b; Thorne and Hardcastle, 1997, Hamilton, 1998; Vincent et al., 1999; Williams et al., 1999; Williams et al., 2000. In the present review just two examples from a tidal estuary and a nearshore wave environment are presented to illustrate the measurement capability and use of the ABS.

4.1.3.1. Tidal estuary. An illustration of results reported from an estuarine environment (Thorne and Hardcastle, 1997) is presented here. The site was the River Taw estuary in North Devon, UK. The estuary was subject to strong tidal currents, which generated high concentrations of fine to medium sand. The instrumentation consisted of a triple frequency ABS operating at 1, 2.5, and 5 MHz, pump sampling, and current meters. The primary aim of the experiment was to assess in the marine environment the implicit iterative inversion algorithm for extracting particle size and concentration. The system was fully electronically and acoustically calibrated thereby allowing suspended sediment concentration and particle size to be obtained independently of pump sampled measurements collected concurrently with the acoustic data. The results of the acoustic inversion and comparison with the pump sampled measurements are shown in Fig. 6. This shows data collected over
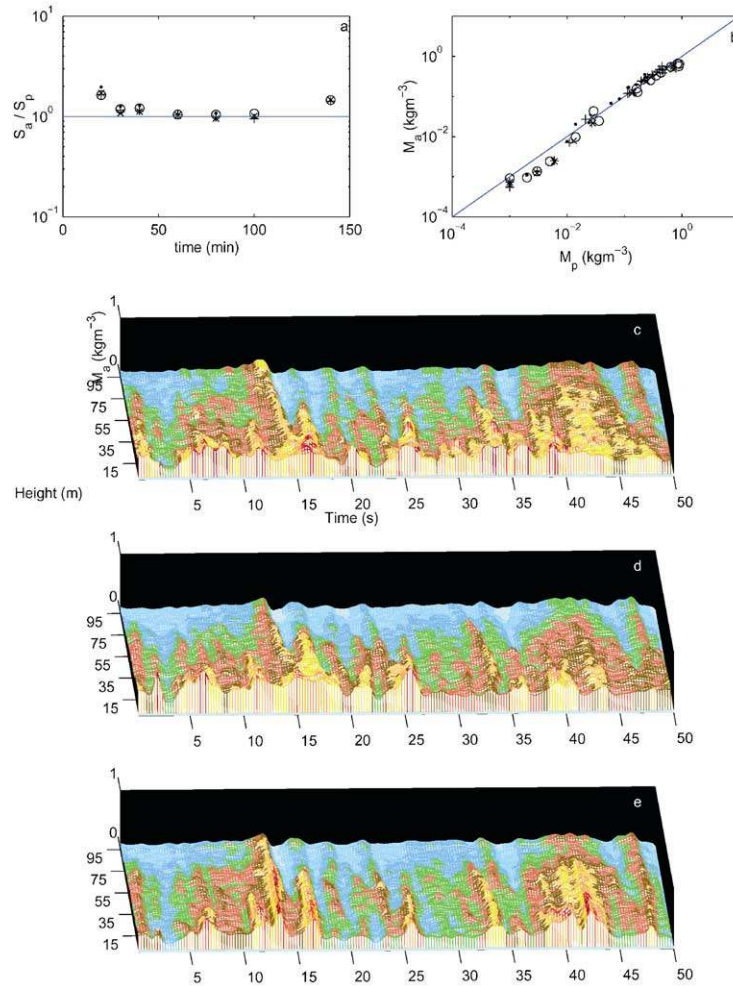
Fig. 6. (a) and (b) are comparisons of the acoustic measurements with the pump sampled size, S_p and concentration, M_p, measurements at; $\bigcirc -0.1$, $\times -0.2$, $+ -0.4$, and $\bullet -0.8$ m above the bed. (c–e) show high temporal resolution measurements of suspended sediment concentration with height above the bed measured at 1, 2.5, 5.0 MHz, respectively.

a flood tide, with peak flow of the order of $1\,\mathrm{ms}^{-1}$ occurring 40 min into the record and slack high water at the end of the record. Fig. 6a shows the acoustic inversion for particle radii, which were nominally $70\,\mu\mathrm{m}$; in the plot the ratio of the acoustic radius, S_a, to the pumped sampled measurements, S_p, is presented. A regression plot of the acoustic, M_a, and the pump sampled, M_p, concentration is shown in Fig. 6b. The data show very encouraging results with the ratio of the acoustic to pump sampled particle size being very

close to unity over most of the flood period, and the gradient from the regression plot of the concentration having a value close to unity. The data shown in Figs. 6a and 6b are, as far as the authors are aware, still the only data where a multifrequency acoustic inversion has been conducted in the marine environment and the results assessed using the absolute reference of pump sampling.

Having ascertained the capability of acoustics to accurately measure suspended sediments,

advantage can be taken of its temporal resolution to probe turbulent resuspension processes. Examples of the results that can be obtained are shown in Figs. 6c–6e. This shows multifrequency high-resolution measurements of the suspended sediment concentration. The internal consistency of the images supports the veracity of the concentration field displayed. It is expected that such visualisations of the form of the suspended sediment concentration, coupled with emerging nearbed velocity profilers, will enhance and develop our understanding of the fundamentals of sediment processes.

4.1.3.2. Nearshore wave dominated environment. Another example of field measurements of suspended concentration using an ABS come from Vincent et al. (1999). They studied the spatial and temporal structure of the concentration of sand suspended above large ripples on a macrotidal beach in Cornwall, England. The goal of the experiment was to measure the processes through which sediment is entrained into suspension above wave formed ripples. To measure the ripples a single ABS transducer was deployed in a sideways looking mode. By ensemble averaging the measurements of fluid velocity and suspended sediment concentration as a function of wave phase for waves of similar size, they generated Fig. 7a, which shows the dramatic difference in the temporal structure of the suspended sediment field over a ripple crest verses over a ripple trough. By making similar observations as the ripple slowly migrated through the measurement region, they also were able to construct the spatial distribution of suspended sediment, as shown in Fig. 7b. These spatial patterns show low concentrations over the ripple crest and high concentrations in the ripple trough during the period of shoreward flow. During the period of seaward flow, the concentration patterns were reversed; there were high concentrations above the ripple crest and low concentrations in the ripple trough. The authors interpreted the temporal and spatial structure to be consistent with the formation of a sediment-laden vortex in the ripple trough during shoreward flow, and the subsequent ejection of this vortex during the following seaward flow. The suspended

sediment concentration profile that results from this process is significantly different than the predictions of models that assume flat bed conditions, and Fig. 7 clearly illustrates the contribution acoustics can make to understanding the processes of sediment transport.

4.2. Acoustic measurements of flow

The success of the acoustic Doppler current profilers, ADCP, which typically provide mean current profiles with decimeter spatial resolution (Brumley et al., 1991) and more recently the acoustic Doppler velocimeter, ADV, which measures three velocity components at a single height (Voulgaris and Trowbridge, 1998), coupled with the development of the ABS, has stimulated interest in using acoustics to measure nearbed velocity profiles. The objective being to use the same backscattered signal as used by the ABS, but process the data to obtain velocity profiles with comparable spatial and temporal resolution to the acoustic backscatter systems. Two emerging approaches that have been demonstrated to have some success in this area are cross-correlation and coherent Doppler, and these are considered in the present work.

4.2.1. Cross-correlation velocity profiler, CCVP
The basic principle of the CCVP is shown in Fig. 8. The figure shows data reported (Taylor et al., 1998; Thorne and Taylor, 2000) from a recent study carried out in the large-scale oscillating wave tunnel at Delft Hydraulics De Voorst Laboratories in the Netherlands. The tunnel had a measurement Section 14 m long, 0.3 m wide, and 1.1 m deep. The facility provided unidirectional, oscillatory and combined flows. The measurements shown in the figure are for unidirectional flow. Fig. 8a and 8b show the backscattered signal from sediments entrained into the water column by the current, for two 2 MHz transducers separated by 0.15 m, aligned along the flow, and directed vertically downwards. Clearly, common features are present in the two figures and close inspection shows the data in Fig. 8b lags 8a by the order of a quarter of a second. The time series signal for each range bin for the transducer pair
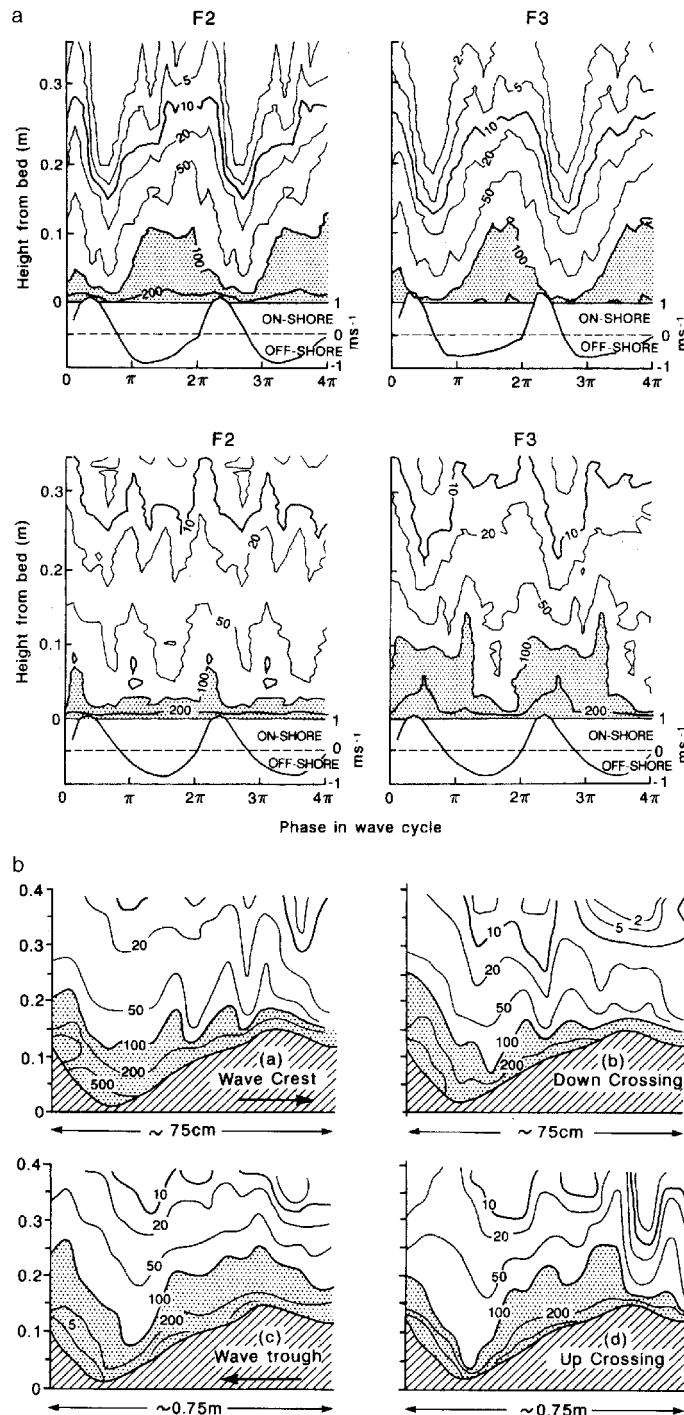
Fig. 7. (a) Acoustic measurements at 4.07 MHz (F2) and 5.57 MHz (F3) of the temporal structure of the suspended sand concentration as a function of the phase of the waves measured (top) over the crest of a megaripple and (bottom) in the trough of a megaripple. The instantaneous current speeds due to the waves are shown below the suspensions. Concentration contours are approximately logarithmic with units of $mg\,l^{-1}$. (b) Spatial suspension patterns over the megaripple over a period of 3 h (a) under the wave crest, (b) downward zero crossing, (c) under the wave trough, and (d) upward zero crossing. Concentration units are in $mg\,l^{-1}$.
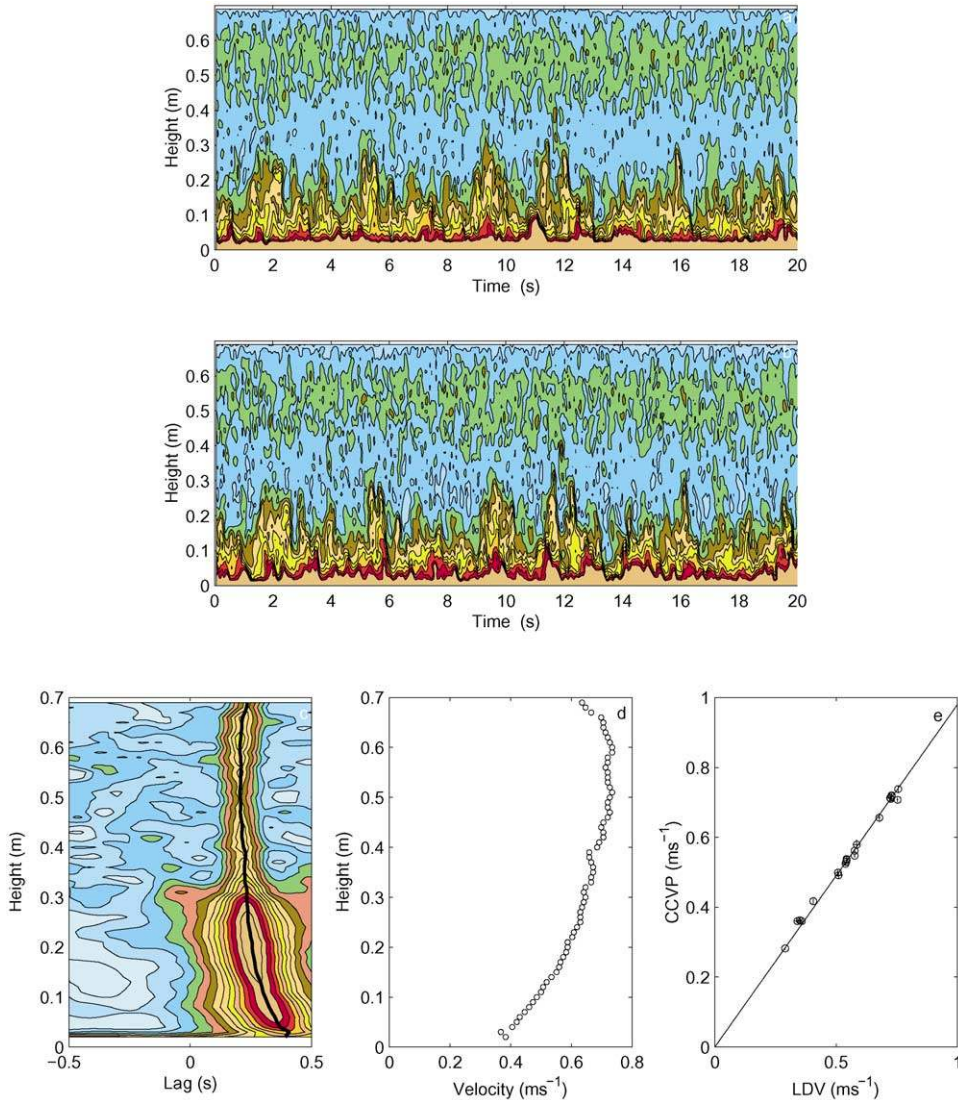
Fig. 8. (a) and (b) Measurements of the backscatter signal from two cross-correlation transducers. (c) The cross-correlation function obtained for each range bin with height above the bed. The solid black line represents the locus of the peaks of the cross-correlation functions. (d) The velocity profile obtained using the cross-correlation method. (e) Regression plot of CCVP and LDV velocity from a number of experimental runs.

were cross-correlated to generate the correlalo-gram shown in Fig. 8c, and using Eqs. (26)–(29), the cross-correlation peak and associated lag were obtained for each range bin and the velocity profile shown in Fig. 8d obtained. The velocity profile shows the expected trend with reductions in flow near the steel plates on the upper surface of the tunnel and towards the sand bed. Measurements were taken for a number of flow rates in the flume, and the results were compared with laser Doppler anomometry, LDV, measurements. The results are shown in Fig. 8e. Normal axis regression analysis

gave $v_c = (0.98 \pm 0.03) v_\ell$ with a regression coefficient of 0.997. v_c and v_ℓ were the cross-correlation and laser velocities, respectively.

To date the published works (van Unen et al., 1998; and Thorne and Taylor, 2000) on the application of cross-correlation velocity profiles in flumes show the technique can accurately measure mean velocity profiles and provide reasonable estimates of period and amplitude under oscillatory flow. Measurements in the field have shown the potential of the technique (Thorne et al., 1998b; Betteridge et al., in press) in unidirectional flow, however, there are no published results showing the outcome of the deployment of a cross-correlation system at sea under waves. The application of the cross-correlation method is still in an evaluation phase and further studies are required to fully establish the capability and limitations of the approach.

4.2.2. Coherent Doppler velocity profiler, CDVP

The CDVP has a longer history of application than the CCVP, with its historical area of use being in the radar field (Doviak and Zrnic, 1993). Recent publications on the application have shown very interesting results in turbulent flow (Zedel and Hay, 1999) including two-component (Rolland and Lemmin, 1997) and three-component flow profiles (Hurther and Lemmin, 1998; Wilson et al., 2000) and some limited measurements under waves (Zedel et al., 1996). The results reported here come from the studies of Hurther and Lemmin, 1998, Zedel and Hay, 1999 and Thorne and Taylor, 2000.

A series of measurements were conducted in the same wave tunnel facility as used for the cross-correlation measurements, using a transducer operating at 524 kHz. An example of the velocity profiles obtained for unidirectional currents is shown in Fig. 9a. The form of the profile is comparable with the CCVP. Regression analysis from a number of experimental runs with LDV measurements gave $v_d = (0.993 \pm 0.03) v_\ell$ with a regression coefficient of 0.994, were v_d was the CDVP velocity. Fig. 9b shows an example of intrawave velocity measurements. The velocities are seen to be very comparable. Measurements of the wave period and amplitude gave 15.96 s and

0.89 m s^{-1} and 15.94 s and 0.89 m s^{-1}, respectively for the CDVP and LDV. Regression of the data gave $v_d = \{1.00 \pm 0.02\} v_\ell$ with a regression coefficient of 0.999. Assessment of the turbulence measuring capability of the CDVP was also conducted and an example of the results is shown in Fig. 9c. The turbulent component is given by $v_i' = v_i - \langle v_i \rangle$ where $\langle v_i \rangle$ was the mean velocity over the record. The CDVP data (blue) is offset by –0.05 m s^{-1} from the LDV data (red). Clearly, the turbulent CDVP and LDV velocities are very comparable. To compare the time series quantitatively, cross-correlation of v_d and v_ℓ was conducted on a number of data sets and the mean of the results with error bars is shown in Fig. 9d. The normalised cross-correlation function has a clear and readily identifiable peak with a maximum value of 0.78. An illustration of the high temporal and spatial resolution profiling capability of the CDVP is shown in Fig. 9e. This shows a three-dimensional visualisation of the turbulent component of flow with height above the bed and time. These images are unique to the profiling capability of the CDVP, and they provide a description of the turbulent flow in the nearbed boundary layer which is a substantial improvement over more conventional measuring techniques. It is anticipated that such measurements will help develop our understanding of the relationship between the turbulent hydrodynamics, and sediment transport processes.

In Figs. 10a and 10b measurements by Zedel and Hay, 1999 and Hurther and Lemmin, 1998 are respectively shown. Fig. 10a shows data collected in 3 m water depth at Queensland Beach, Nova Scotia, Canada. The 1.7 MHz acoustic profiler utilised the rate of change of phase and amplitude of the backscattered signal, to obtain high temporal resolution velocity and suspended sediment concentration, collocated and with subcentimeter resolution. This direct measurement of sediment flux, and the wealth of detail shown in such images, should contribute significantly to developing our understanding of sediment transport processes. The very high resolution measurements shown in Fig. 10b were obtained using a 1 MHz focused transmitting transducer with four receivers. The data were collected in an open
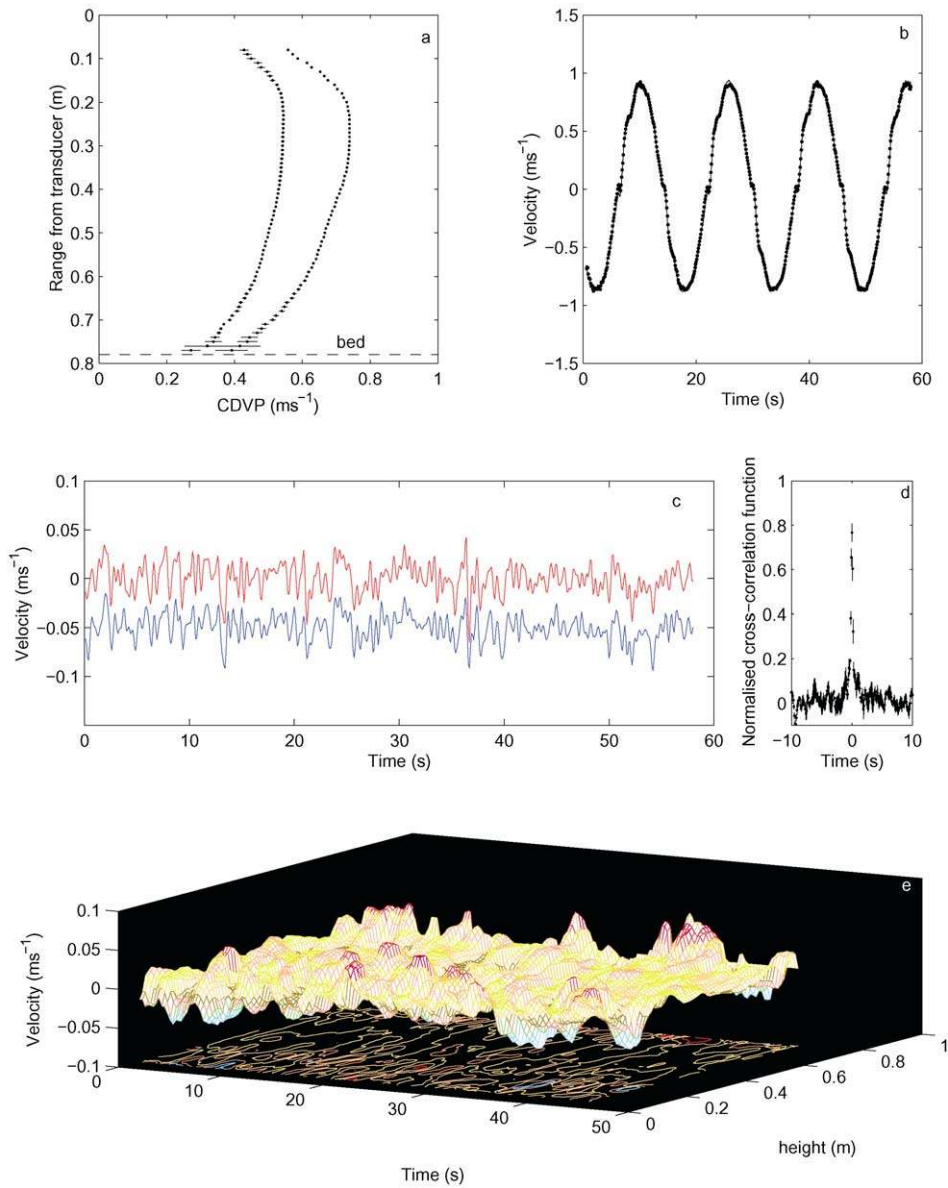
Fig. 9. (a) Velocity profile measurements obtained with CDVP in unidirectional flow. (b) Intra-wave velocities obtained from the LDV (−) and CDVP (·). (c) Comparison of turbulent velocity measurements obtained from the LDV (red line) and CDVP (blue line). The CDVP measurements have been offset by $-0.05\,\mathrm{m\,s^{-1}}$. (d) Cross-correlation of the LDV and CDVP turbulent velocity measurements. (e) Variation of the turbulent velocity with height above the bed and time.

channel laboratory flume with unidirectional flow. The system provides profiles of the three orthogonal flow components. The figure shows the two-dimensional velocity vector $V'\{u'(t); w'(t)\}$, where u' and w' are the fluctuating components of the horizontal and vertical flow velocity. The velocity measurements were at 10 Hz and clearly demonstrate organised behaviour in the turbulent flow.
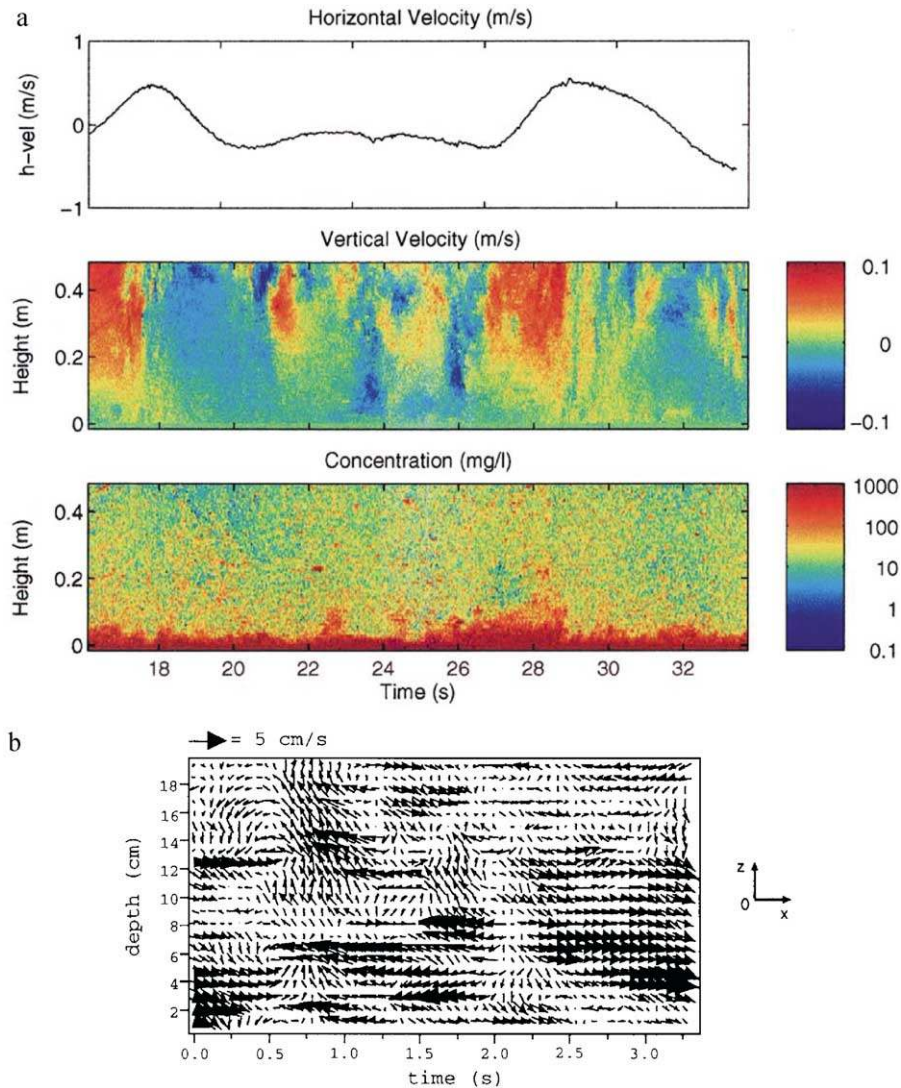
Fig. 10. (a) Acoustic measurements of horizontal flow, vertical flow, and suspended sediment concentration obtained in 3 m deep water 60 m offshore in the bottom boundary layer, Zedel and Hay, 1999. (b) Time series of the two-dimensional velocity vector $V'\{u'(t); w'(t)\}$ with 10 Hz resolution, Hurther and Lemmin, 1998.

These three axis velocity profilers, coupled with backscatter amplitude measurement for suspended sediment observations, are beginning to provide a powerful research tool for hydrodynamic and sediment studies.

The measurements presented here and those of other referenced studies clearly show the capability of the CDVP to accurately measure mean, turbulent and oscillatory flow. There is the problem with CDVP of velocity aliasing, however, there are such techniques as interleaved alternating pulse repetition frequencies and other methods which should be able to overcome this problem (Brumley et al., 1991). The laboratory studies and limited marine measurements carried out to-date show the potential of CDVP, and no doubt in the

near future repeated usage of the technique at sea will provide the measurements to assess whether this potentiality can be fully realised.

4.3. Measurements of bed morphology

To complete the triad of measuring the suspended sediments, hydrodynamics, and the bedform morphology, systems have recently been developed to measure local seabed morphology with subcentimeter resolution. The form of the bed significantly affects the distribution of the suspended sediments with height above the bed, and is therefore a central component in sediment entrainment and transport. To date high resolution morphological measurements have been collected by simply directing an ABS at low grazing angles towards the bed (Vincent and Osborne, 1993) and recording the return echo, or by developing systems specifically designed to measure the bedform details (Hay and Wilson, 1994; Jette and Hanes, 1997). The specifically designed systems typically either provide quantitative measurements of the evolution of a bed profile with time, or generate an image over an area of the local bed features. For the convenience of discussion we will use the nomenclature of calling the former bed ripple profilers and the latter bed ripple scanners.

4.3.1. Bed profilers

To date the bed ripple profilers reported have been of one of three types; (i) a single transducer pointing vertically down towards the bed, which is physically translated along the profile to make a measurement (Greenwood et al., 1993), (ii) a multi-transducer linear array which provides measurements along a transect (Jette and Hanes, 1997), and (iii) a single transducer which radially rotates to provide a profile of the bed (Bell and Thorne, 1997; Bell et al., 1998). The single transducer has the virtue of simplicity and its use has been demonstrated, however, the mechanics of such a system may make its general deployment in the marine environment problematic. The linear transducer array overcomes the mechanical problems, although with some increased electronic complexity, however, given present day processing

capability this is not an impediment. The radially rotating transducer preserves the simplicity of using a single transducer, but does require relatively sophisticated hardware and software, however, the systems are now commercially available and can be readily obtained (Collier, 1999).

An example of a multiple transducer array, MTA, has been reported by Jette and Hanes (1997). The MTA reported here consisted of thirty-seven 0.01 m diameter disc elements operating at 5 MHz. The separation of the centre of the discs was 0.02 m and the transducer array was 0.64 m in length, 0.08 m in width and 0.02 m in height. To establish the capabilities of the MTA, a template was constructed to enable the creation of a sand bed ($D_{50} = 0.1$ mm) with bedforms comparable to those observed in the field. The results of direct physical and acoustic measurements are shown in Fig. 11a. The root-mean-square difference between the MTA and the direct measurements was 0.008 m. For smooth sloping beds or beds with only small scale ripples the root-mean-square difference was typically less, while the accuracy of the MTA degraded slightly for a combination of large and small-scale ripples because of the more extreme slopes that occurred. As part of the SISTEX99 experiment described in Section 4.1.2, the MTA was deployed for bedform measurements. The MTA was mounted on a moving carriage 0.4 m above the bed and profiles collected under a number of wave conditions over the 40 m sand bed section. Examples of bedform profile measurements are shown in Figs. 11b and 11c. The rippled bed shown in Fig. 11b was formed with a water depth of 4 m under monochromatic waves with a period of 6.5 and a height of 1.0 m. The relatively smooth seabed shown in Fig. 11c corresponds to nominally sheet flow sediment transport conditions. This seabed was formed in a water depth of 3.5 m by monochromatic waves with a period of 9.1 s and a height of 1.5 m. It is quite clear that the two wave conditions have significantly different bed features that were clearly identified by the MTA. Fig. 11d shows data collected with a 2 MHz rotating ripple profiler in the nearshore environment. Comparison of the output from the ripple profiler with a
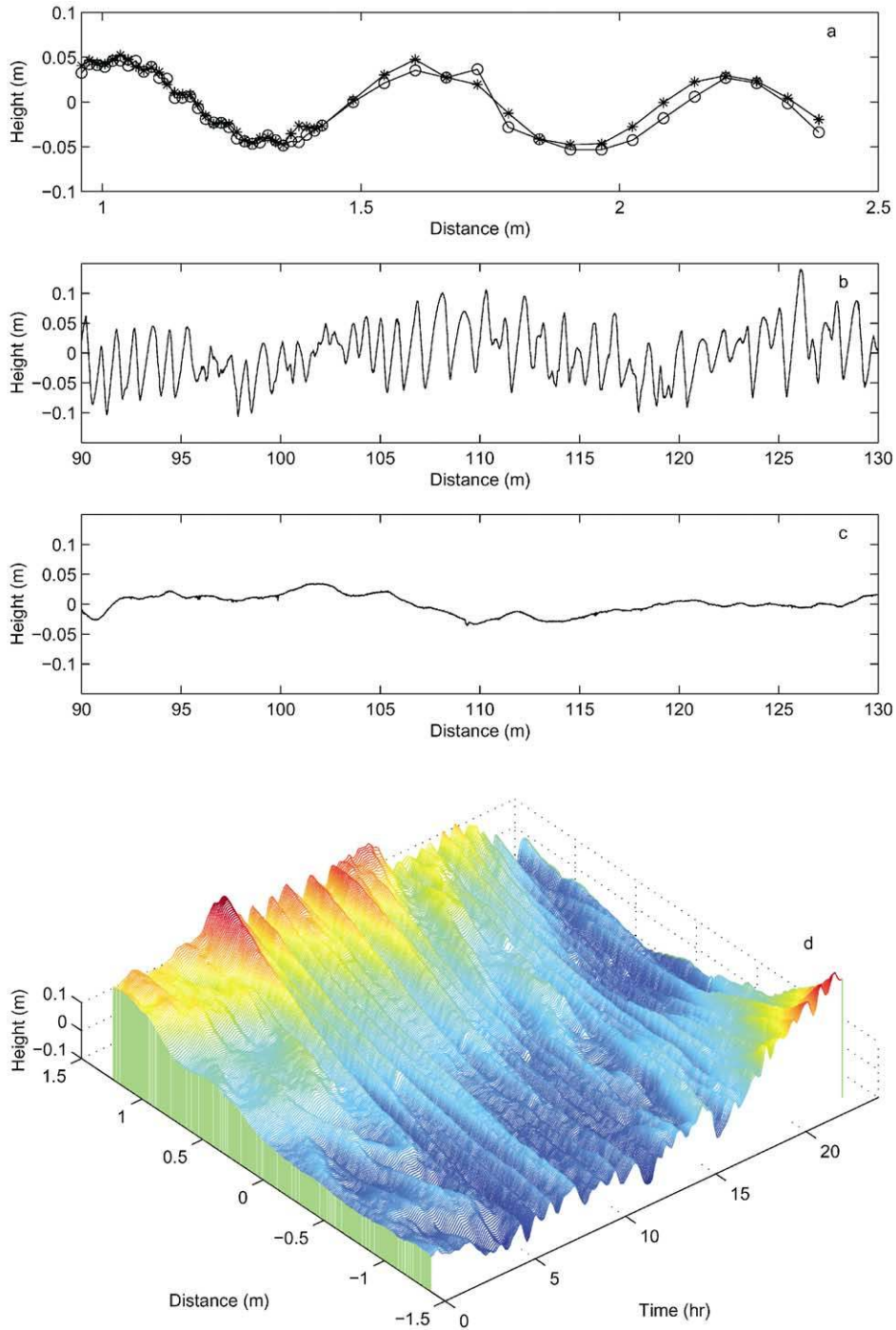
Fig. 11. (a) Bed profile measurements obtained in the laboratory with an MTA ($\bigcirc$) and manually with a ruler (*); (b) and (c) Examples of a rippled bed and flat bed profile from SISTEX99 as measured with a translating MTA. (d) Ripple profiler measurements collected at sea of a transect over a period of 24 h.

known surface indicated an accuracy of around ± 0.005 m (Bell and Thorne, 1997). The figure shows the bedform variability over nominally a 3 m transect covering a 24 h period. Over this period the bed was subject to both tidal currents and waves and the figure shows the complex evolution of the bed with periods of ripples and less regular bedforms.

4.3.2. Bed scanners

Ripple scanners are based on sector scanning technology that has been specifically adapted for high resolution images of bedform morphology. They typically have a frequency of around 2 MHz with beam widths of about $1°$ in the azimuth and $30°$ in elevation. As the pulse is backscattered from the bed, the envelope of the signal is measured and usually displayed as image intensity. Examples of a seabed imaging systems can be found in Hay and Wilson, 1994; Hume et al., 1999; Irish et al., 1999; Traykovski et al., 1999 and Williams et al., 2000. Traykovski et al. (1999) deployed a sector scanning sonar in a medium-to-coarse sand environment in 11 m depth off the coast of New Jersey. During a series of storms they observed the evolution of the seabed, as well as other aspects of small-scale sediment transport using an ABS and other instrumentation. Fig. 12 (extracted from their original Fig. 6) show a series of acoustic images of the seabed over a 2-day period. The root-mean-square wave velocity and the current velocity are also shown in the small plot in the upper left of each image. In the first image, the seabed exhibits relic ripples left from a previous storm. During day 239, as the waves increase, the bed forms three-dimensional ripple patterns, followed during day 240 by regular two-dimensional vortex ripples. Traykovsky et al., have interpreted these data along with other observations, and provided a thorough and intriguing description of the evolution of seabed morphology during a series of storm events.

4.4. An integrated approach

As mentioned earlier, the vision of over a decade ago was to utilise acoustics to measure the three components of suspended sediment, flow and

bedform morphology contemporaneously and co-located. Only a few reports (Traykovski et al., 1999, Betteridge et al., in press) have included a combinations of systems. In the present article results are reported from a study conducted in the River Taw estuary, UK, (Thorne et al., 1998a) where triple frequency ABS, CDVP, CCVP and ripple profiling data were collected together. The reference instruments for measuring the flow were electromagnetic, rotor, and ADV current meters, and for the suspended sediment concentration pump sampling at 0.1, 0.2, 0.4 and 0.8 m above the bed.

To evaluate the ABS data the explicit inversion algorithm was used with the pump sampled data collected at 0.1 m above the bed. The mean particle size from this study and others (Thorne and Hardcastle, 1997) at the same location had showed the particle size was nominally constant above approximately 0.05 m above the bed and therefore Eq. (21) was used for the inversion. The results are shown as a regression plot of M_a the acoustic concentration, and M_p, the pump sampled concentration, in Fig. 13a. Regression analysis on the data gave a regression coefficient of 0.98, and $M_a = (1.06 \pm 0.05)M_p$. The acoustic and pumped sampled concentrations were therefore very comparable. To assess the capability of CDVP and the CCVP in the marine environment, comparisons of the velocity measured at the range coincident with the location of the ADV measurements were presented. The results are shown in Figs. 13b and 13c. Figs. 13b shows a regression plot for the CDVP and the ADV. This gave a regression equation of $v_d = (-0.01 \pm 0.01) + (1.03 \pm 0.02)V_{adv}$ with a regression coefficient of 0.999. Essentially there was no significant difference between the CDVP and the ADV. The comparable analysis in Fig. 13c with the CCVP and the ADV gave $v_c = (0.03 \pm 0.07) + (0.99 \pm 0.1)V_{adv}$ with a regression coefficient of 0.92. As with CDVP there is no significant difference between the CCVP and the ADV, however, there is greater scatter in the data, which may be an indication of the possible limitations of the cross-correlation technique. To complete the trio of suspended sediment, flow and bed measurements, a ripple profiler was used to identify the time history of a profile along the bed
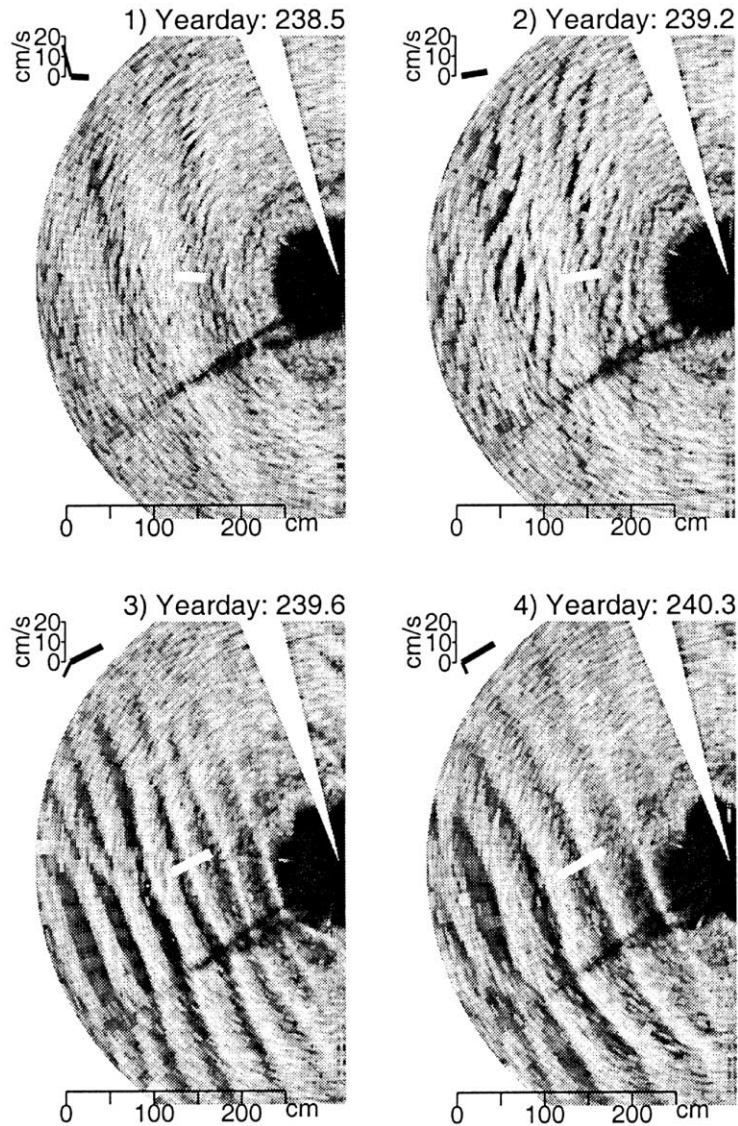
Fig. 12. Sector-scanner images of the bed from Traykovski et al., 1999. The thick white line near the centre of each image represents the wave orbital diameter scaled by 3/4 and is aligned in the wave direction. The small plot in the upper left of each image displays the relative wave rms velocity (thick line) and current velocity (thin line).

in the flow direction. Fig. 13d shows the measurements obtained. At the beginning of the flood tide, small progressive sand ripple features can just be made out on the sandwave. As the flow increased towards maximum, approximately $1\,\mathrm{m\,s^{-1}}$, there is seen to be a rapid reduction in bed height as the sandwave migrated beneath the frame. As the flow

reduced there was no further variation in sandwave height, however, ripples are seen to form and migrate over the sandwave which finally remain fixed in location as slack high water was reached at the end of the flood tide. Integration of the three components is shown in Fig. 13e. The CDVP and the ABS have been combined to obtain suspended
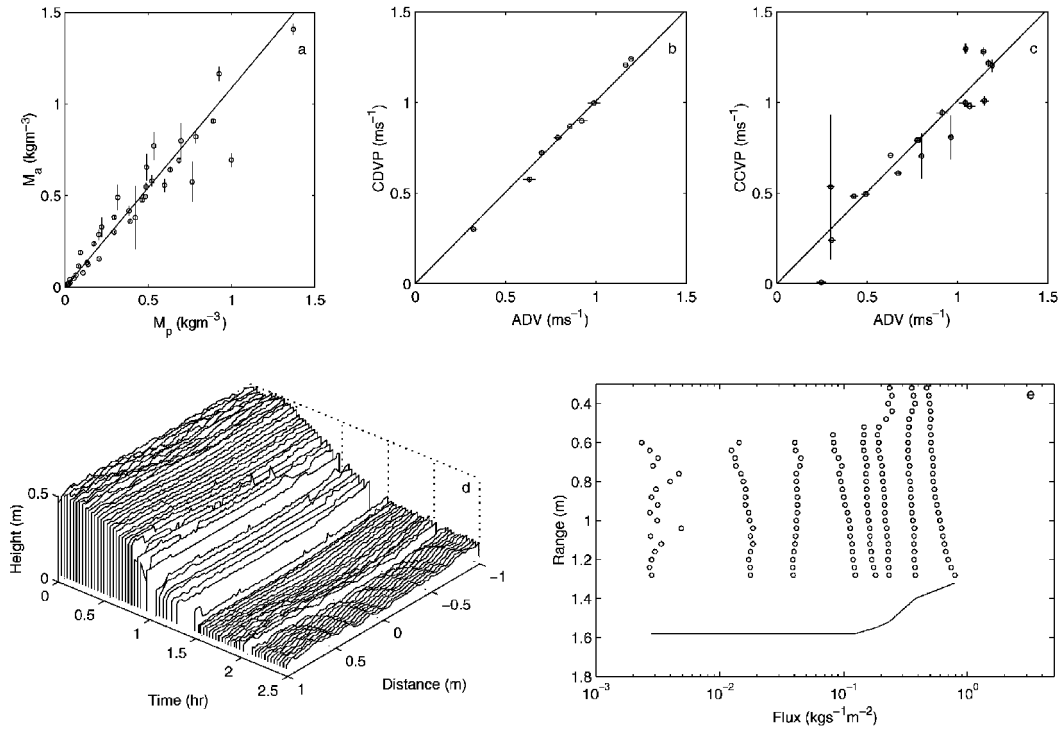
Fig. 13. (a) Regression plot of the acoustic, M_a, and the pump sampled M_p, concentrations. (b–c) Regression plots of the CDVP and CCVP with the ADV. (d) Ripple profiler measurement of the bed. (e) Measurements of the variation of flux with height above the bed over the flood period.

sediment flux profiles, $S_f(r) = M_a(r)v_d(r)$, using mean current and concentration profiles. The flux profiles are shown above the location of the bed, with the profiles on the right of the figure collected near maximum flow and progressively moving towards the left of the figure as slack high water was approached. Unfortunately due to the migration of the sandwave beneath the instruments, the bed fell below the maximum range bin of the CDVP. However, the principle of integrated measurements is illustrated in the figure; bedform morphology, concentration and flow profiles, and their combination to give flux profiles.

5. Discussion and conclusions

The aim of the present work has been to outline the acoustic techniques developed over recent

years for studying small-scale sedimentation processes. This application of acoustics is still in an ongoing developmental phase and there are limitations and shortcomings that need to be overcome, and further applications explored. Presented in this section is a brief discussion regarding present limitations, and the requirement for future developments.

5.1. Morphology

In the text results from recently developed scanning and profiling systems have been presented. The profilers to date only operate along a single transect, and therefore in the simple case of a two-dimensional ripple field, if the transect is not orthogonal to the direction of the ripples, erroneous ripple wavelengths would be measured. Scanners can put the profile measurements into

context, however, the scanner images themselves are relatively qualitative in nature, and with spatial coverage which can be limited by shadow zones at low grazing angles. Further, significant levels of scatterers in the water column can make the location of the bed from ripple profilers problematic and deteriorate the images from scanners. There is certainly the requirement to develop a ripple profiling system capable of covering an area with a sophisticated bed location and tracking system. Such systems would provide detailed quantitative topographic measurements of the local bedform morphology over several square metres. One can readily envisage how the MTA and the radial ripple profilers could be adapted to provide quantitative four dimensional measurements (three space and time), and if given sufficient priority it is fully anticipated that new acoustical/mechanical designs over the next few years could provide a four dimensional bedform profiling system.

5.2. Flow

The application of coherent Doppler and cross-correlation methods has recently emerged for measuring velocity profiles with the spatial and temporal resolution required for small-scale process studies. The CCVP and CDVP have both now been extensively scrutinised in the laboratory, with some limited assessments in the field. The results of some of these measurements have been referred to here. One concern regarding the measurement of the flow using acoustics is that the systems rely on the scattering of sound by discrete scatterers, the velocities of which are used to infer the water velocity. For small size sediment scatterers or microbubbles the particle motions will be very comparable to that of the fluid, however, for larger scatterers there certainly exists the potential for error, particularly if the principle interest is in the measurement of turbulence and Reynold stress. It would therefore seem desirable to obtain concurrent particle size information, (which could be acoustically obtained) and incorporate it into the processing of the velocity data.

The results in the present article have been primarily focussed on measuring velocity profiles in a single direction, but reference (Hurther and Lemmin, 1998; and Wilson et al., 2000, Zedel and Hay, submitted for publication) has been made to Doppler systems that can provide simultaneous and collocated profiles of the three orthogonal components of flow. These developing Doppler systems, which use a combination of narrow circular beam and fan beam transducers, appear to be the next stage in the development of the Doppler systems. Nevertheless it should be noted that the maximum range-velocity ambiguity of Eq. (25) does impose system limits, and methodologies are required to overcome this problem to establish a more generic use for coherent Doppler systems. The extension of the CCVP technique beyond its present stage to obtain mean velocity profiles of the two horizontal components of flow using transducers on orthogonal crosslines appears practicable, however, no such measurements have been reported to date.

5.3. Concentration

It was from the concept of using acoustics to measure suspended sediment concentration that its application to the other components of the small-scale sedimentation processes triad followed. To date the use of sound to measure suspended sediment concentration and particle size has been successful when systems have been deployed over seabeds of nominally homogeneous non-cohesive sediments. This success is associated with laboratory and theoretical studies that have been conducted over a number of years, and have established a framework which describes at least to first order the scattering properties of inorganic quartz based sediments. However, all who use acoustics recognise that the marine sedimentary environment is frequently much more complicated, and suspensions of cohesive sediments and combined cohesive and non-cohesive sediments are common. Also the presence of biological material and bubbles can contaminate the backscattered signal. The latter point is of particular importance owing to the resonant nature of bubbles leading to acoustic cross-sections which are significantly greater than their physical dimensions (Leighton, 1994; Medwin and Clay, 1998).

There are few bubble measurements in the nearshore zone during high energy events owing to the extremely challenging physical conditions. The limited measurements reported (Deane, 1997; Leighton et al., 2001) do show high concentrations of bubbles over a broad radius distribution, 10–1000 μm, with corresponding resonance frequencies of 300 kHz–3 kHz. There are no measurements of the bubble population below 10 μm and it is therefore not possible to assess the resonance effect on the megahertz frequencies normally used for ABS systems. However, normal geometric scattering by bubbles will make the use of acoustics for the measurement of sediment transport processes in the dynamic breaking wave zone problematic, although Schat (1997) claimed success in the measurement of suspended sediments in the surf zone.

To resolve some of the difficulties described above requires the establishment of a description of the scattering properties of suspensions of cohesive sediments and sediment mixtures. This would be interesting and very valuable work, and should significantly extend the deployment regime over which acoustic backscattering can be employed quantitatively. As well as understanding the acoustic scattering properties of more complex suspensions there is the requirement to advance the inversion methodologies used to translate the backscattered signal to suspension parameters. Present inversion algorithms have a tendency to become unstable when sediment attenuation becomes substantial (Thorne and Hardcastle, 1997). The bed echo has been used to constrain the inversion (Thorne et al. (1995b)) and least mean square compensation algorithms (Shen and Lemmin, 1998; Thosteson and Hanes, 1998) have been utilised, however, these are only the first steps towards making the inversion methodologies more robust. The inversion algorithms used in electromagnetics may provide some valuable pointers to advancing the inversion approaches used in acoustics. Radar has been used for over two decades (Testud et al, 2000) both terrestrially and from space to probe precipitation, and measure such parameters as rainfall rate and droplet size. These methodologies may have an acoustic analogue (Humphery and Zhang, 2000).

Finally, although one could extend the above discussions, they are presented simply as an illustration of some of the difficulties of employing acoustics, the gains, and the possible areas of future development. The primary objective of the paper has been to attempt to clarify the role of acoustics, coupled with the underlying physics and methodologies, as a technique for sedimentation studies. It is clearly acknowledged that acoustics is one of a number of technologies advancing our capabilities to probe sediment processes. However, its non-intrusive profiling capability coupled with its potential to measure all three components of the sediment dynamics triad make it a very powerful tool for examining small-scale sediment transport processes.

Acknowledgements

References

Agrawal, Y.C., Pottsmith, H.C., 1993. Optimising the kernel for laser diffraction particle sizing. Applied Optics 32 (22), 4285–4286.

Agrawal, Y.C., Pottsmith, H.C., 1994. Laser diffraction particle sizing in STRESS. Continental Shelf Research 14 (10/11), 1101–1121.

Agrawal, Y.C., Pottsmith, H.C., 2000. Instruments for particle size and settling velocity observations in sediment transport. Marine Geology 168, 89–114.

Bell, P.S., Thorne, P.D., 1997. Application of a high resolution acoustic scanning system for imaging sea bed microtopography. Seventh International Conference on Electronic Engineering in Oceanography. Held at the Southampton Oceanographic Centre 23–25 June 1997. IEE Conference Publication No. 435, 128–133.

Bell, P.S., Thorne, P.D., Williams, J.J., 1998. Acoustic measurements of sand ripple profile evolution under controlled wave conditions. Proceedings of the Fourth European Conference on Underwater Acoustics, held in Rome, Vol.1, September 21–25 1998, pp. 353–358.

Betteridge, K.F.E., Thorne, P.D., Bell, P.S. Assessment of acoustic coherent Doppler and cross-correlation techniques for measuring near-bed velocities and suspended sediment profiles in the marine environment. Journal of Atmospheric and Oceanic Technology, in press.

Brumley, B.H., Cabrera, R.G., Deines, K.L., Terray, E.A., 1991. Performance of a broad-band acoustic Doppler current profiler. IEEE Journal of Oceanic Engineering 16 (4), 402–407.

Bunt, J.A.C., Larcombe, P., Jago, C.F., 1999. Quantifying the response of optical backscatter devices and transmiss-ometers to variations in suspended particulate matter. Continental Shelf Research 19, 1199–1220.

Cheng, H., Hay, A.E., 1993. Broadband measurements of the acoustic backscatter cross section of sand particles in suspension. Journal of the Acoustical Society of America 94 (4), 2247–2254.

Clarke, T.L., Proni, J.R., Craynock, J.F., 1984. A simple model for the acoustic cross section of sand grains. Journal of the Acoustical Society of America 76, 1580–1582.

Collier, G., 1999. Marine Electronics Ltd., Unit10, Barras Lane Industrial Estate, Vale, Guernsey, C.I., GY6 8EQ. Tel.: +44-(0)-1481-253181, Private communications, 1999.

Crawford, A.M., Hay, A.E., 1993. Determining suspended sand size and concentration from multifrequency acoustic back-scatter. Journal of the Acoustical Society of America 94 (6), 3312–3324.

Deane, G.B., 1997. Sound generation and air entrainment by breaking waves in the surf zone. Journal of the Acoustical Society of America 102 (5) (Pt. 1) 2671–2689.

Doviak, R.J., Zrnic, D.S., 1993. Doppler Radar and Weather Observations. Academic Press, New York, pp. 562.

Downing, J.P., Sternberg, R.W., Lister, C.R.B., 1981. New instrumentation for the investigation of sediment suspen-sion processes in the shallow marine environment. Marine Geology 42, 19–34.

Downing, A., Thorne, P.D., Vincent, C.E., 1995. Backscatter-ing from a suspension in the nearfield of a piston transducer. Journal of the Acoustical Society of America 97, 1614–1620.

Gallagher, E.L., Elgar, S., Thornton, E.B., 1998. Megaripple migration in a natural surf zone. Nature 394, 165–168.

Green, M.O., Dolphin, T.J., Swales, A., Vincent, C.E., 1999. Transport of mixed-size sediments in a tidal channel. Coastal Sediments'99, pp. 645–658.

Greenwood, B., Richards, R.G., Brander, R.W., 1993. Acoustic imaging of sea-bed geometry: a high resolution remote tracking sonar (HRRTS II). Marine Geology 112, 207–218.

Hamilton, L.J., 1998. Calibration and interpretation of acoustic backscatter measurements of suspended sediment concen-tration profiles in Sydney Harbour. Acoustics Australia 26 (3), 87–93.

Hanes, D.M., 1991. Suspension of sand due to wave groups. Journal of Geophysical Research 96 (C5), 8911–8915.

Hanes, D.M., Vincent, C.E., 1987. Detailed dynamics of nearshore suspended sediments. In: Kraus, N.C. (Ed.), Coastal Sediments 1987. American Society of Civil Engineers, New Orleans, LA, pp. 258–299.

Hanes, D.M., Vincent, C.E., Huntley, D.A., Clarke, T.L., 1988. Acoustic measurements of suspended sand concentration in the C^2S^2 experiment at Stanhope Land, Prince Edwards Island. Marine Geology 81, 185–196.

Hardcastle, P.J., 1995. A high resolution coherent acoustic Doppler profiler for the measurement of near bed turbulent flow. Proceedings Oceans 95, New York, pp. 1361–1366.

Hay, A.E., 1991. Sound scattering from a particle-laden turbulent jet. Journal of the Acoustical Society of America 90, 2055–2074.

Hay, A.E., Bowen, A.J., 1994. Coherence scales of wave-induced suspended sand concentration fluctuations 99 (C6), pp. 12 749–12 765.

Hay, A.E., Sheng, J., 1992. Vertical profiles of suspended sand concentration and size from multifrequency acoustic back-scatter. Journal of Geophysical Research 97 (C10), 15661–15677.

Hay, A.E., Wilson, D., 1994. Rotary sidescan images of nearshore bedform evolution during a storm. Marine Geology 119, 57–65.

Holdaway, G.P., Thorne, P.D., 1997. Determination of a fast and stable algorithm to evaluate suspended sediment parameters from high-resolution acoustic backscatter sys-tems. Seventh International Conference on Electronic Engineering in Oceanography, held at Southampton Ocea-nography Centre, UK, 23–25 June, pp. 86–92.

Hume, T.M., Green, M.O., Oldman, J.W., 1999. What happens at the seabed off a headland during a tropical cyclone. Coastal Sediments'99, pp. 1836–1851.

Humphery, V.H., Zhang, J., 2000. Inversion of multifrequency backscatter data to obtain suspended sediment size and concentration. In: Manell E. Zakhatia (Eds.), Proceedings of the Fifth European Conference on Underwater Acoustics ECUA 2000, Vol. 2. Lyon, France 10–13 July 2000. EU, Luxembourg, pp. 801–806.

Hurther, D., Lemmin, U., 1998. A Constant-beam-width transducer for 3D acoustic Doppler profile measurements in open-channel flows. Measures in Science and Technology 9, 1706–1714.

Irish, J.D., Lynch, J.F., Traykovski, P.A., Newhall, A.E., Prada, K., Hay, A.E., 1999. A self-contained sector-scanning sonar for bottom roughness observations as part of sediment transport studies. Journal of Atmospheric and Oceanic Technology 16 (11), 1830–1841.

Jansen, R.H., 1979. An Ultrasonic Doppler Scatterometer for Measuring Suspended Sand Transport. In: Novak, Z (Ed.), Ultrasonic International 79, Conference Proceedings. Graz, Austria, UI 79, pp. 336–369.

Jette, C.D., Hanes, D.M., 1997. High-resolution sea-bed imaging: an acoustic multiple transducer array. Measures in Science and Technology 8, 787–792.

Kaye, G.W.C., Laby, T.H., 1986. Tables of Physical and Chemical Constants. Longman, UK, pp. 477.

Lee, T.H., Hanes, D.M., 1995. Direct inversion method to measure the concentration profile of suspended particles using backscattered sound. Journal of Geophysical Research 100 (C2), 2649–2657.

Lee, T.H., Hanes, D.M., 1996. Comparison of field observations of the vertical distribution of suspended sand and its prediction by models. Journal of Geophysical Research 101 (C2), 3561–3572.

Leighton, T.G. 1994. The Acoustic Bubble. Academic Press Ltd, London, pp. 613.

Leighton, T.G., Meers, S.D., Simpson, M.D., Clarke, J.W.L., Yim, G.T, Birkin, P.R., Watson, Y.E., White, P.R., Heald, G.J.,Dumbrell, R.L.,Culver, R.L., Richards, S.D., 2001. The Hurst Spit experiment: the characterisation of bubbles in the surf zone using multiple acoustic techniques. In Conference held at the Southampton Oceanographic Centre 9–12 April 2001. Acoustical Oceanography 23 (2), 227–234.

Lemmin, U., Rolland, T., 1997. Acoustic velocity profiles for laboratory and field studies. Journal of Hydraulic Engineering 123 (12), 1089–1098.

Lhermitte, R., Lemmin, U., 1994. Open-channel flow and turbulence measurement by high-resolution Doppler sonar. Journal of Atmospheric Oceanic Technology 11, 1295–1308.

Libicki, C., Bedford, K.W., Lynch, J.F., 1989. The interpretation and evaluation of a 3-MHz acoustic backscatter device for measuring benthic boundary layer sediment dynamics. Journal of the Acoustical Society of America, Vol. 85, No. 4 1501–1511.

Ludwig, K.A., Hanes, D.M., 1990. A laboratory evaluation of optical backscatterance suspended solids sensors exposed to sand-mud mixtures. Marine Geology 94, 173–179.

Lynch, J.F., Gross, T.F., Brumley, B.H., Filyo, R.A., 1991. Sediment concentration in HEBBLE using a 1-MHz acoustic backscatter system. Marine Geology 99, 361–385.

Lynch, J.F., Irish, J.D., Sherwood, C., Agrawal, Y.C., 1994. Determining suspended sediment particle size information from acoustical and optical backscatter measurements. Continental Shelf Research 14 (10/11), 1139–1165.

Lynch, J.F., Gross, T.F., Sherwood, C.R., Irish, J.D., Brumley, B.H., 1997a. Acoustical and optical backscatter measurements of sediment transport in the 1988–1989 STRESS experiment. Continental Shelf Research 17 (4), 337–366.

Lynch, J.F., Irish, J.D., Gross, T.F., Wiberg, P.L., Newhall, A.E., Traykovski, P.A., Warren, J.D., 1997b. Acoustic measurements of the spatial and temporal structure of the near-bottom boundary layer in the 1990–1991 STRESS experiment. Continental Shelf Research 17 (10), 1271–1295.

Medwin, H., Clay, C.S., 1998. Fundamentals of Acoustical Oceanography. Academic Press, New York, pp. 712.

Osbourne, P.D., Vincent, C.E., 1996. Vertical and horizontal structure in suspended sand concentration and wave-induced fluxes over bedforms. Marine Geology 115, 207–226.

Richards, S.D., Heathershaw, A.D., Thorne, P.D., 1996. The effect of suspended particulate matter on sound attenuation in seawater. Journal of the Acoustical Society of America 100 (3), 1447–1450.

Rolland, T., Lemmin, U., 1997. A two-component acoustic velocity profiler for use in turbulent open-channel flow. Journal of Hydraulic Research 35 (4), 545–562.

Schaafsma, A.S., 1995–1998. Private communication. Measurements supplied as part of an EU programme TRIDISMA, MAST-CT95-0017, conducted between, 1995–1998.

Schaafsma, A.S., Kinderen, W.J.G.J., 1985. Ultrasonic instruments for the continuous measurement of suspended sand transport. In: Wessels, A.C.E. (Ed.), Proceedings of the IHAR Symposium on Measuring Techniques in Hydraulic Research held at Delft Hydraulics 22–24 April 1985. A. A. Balkema, Rotterdam, 1986, pp. 125–136.

Schaafsma, A.S., Hay, A.E., 1997. Attenuation in suspensions of irregularly shaped sediment particles: a two-parameter equivalent spherical scatterer model. Journal of the Acoustical Society of America 102 (3), 1485–1502.

Schat, J., 1997. Multifrequency acoustic measurement of concentration and grain size of suspended sand in water. Journal of the Acoustical Society of America 101 (1), 209–217.

Shen, Lemmin, 1998. Improvements in acoustic sediment concentration profiling using an LMS compensation algorithm. IEEE Journal of Oceanic Engineering 23 (2), 96–104.

Sheng, J., Hay, A.E., 1988. An examination of the spherical scatterer approximation in aqueous suspensions of sand. Journal of the Acoustical Society of America 83, 598–610.

Sheng, J., Hay, A.E., 1995. Sediment eddy diffusivities in the nearshore zone, from multifrequency acoustic backscatter. Continental Shelf Research 15 (2/3), 129–147.

Smerdon, A.M., Aquatec Electronics limited, High Street, Hartley Wintney, Hants, RG27 8NY, UK. Tel.: +44 (0) 1252 843072, Private communication, 1998.

Sternberg, R.W., Kineke, G.C., Johnson, R., 1991. An instrument system for profiling suspended sediment, fluid and flow conditions in shallow marine environments. Continental Shelf Research 11, 109–122.

Taylor, J.A., Vincent, C.E., Thorne, P.D., Hardcastle, P.J., Humphrey, V.F., Zhang, J.D., Schaafsma, A., Dohmen-Janssen, C.M., Perennes, M., 1998. Three-dimensional sediment transport measurements by acoustics (TRIDISMA). In: Oceans '98 Conference proceedings, Vol. 228, September–1 October 1998. Nice, France. IEEE/OES, New Jersey (1853pp), pp. 1108–1114.

Testud, J., Le Bouar, E., Obligis, E., Ali-Mehenni, M., 2000. The rain profiling algorithm applied to polarimetric weather radar. Journal of Atmospheric and Oceanic Technology 17, 332–356.

Thorne, P.D., Campbell, S.C., 1992. Backscattering by a suspension of spheres. Journal of the Acoustical Society of America 92, 978–986.

Thorne, P.D., Hardcastle, P.J., 1997. Acoustic measurements of suspended sediments in turbulent currents and comparison with in-situ samples. Journal of the Acoustical Society of America 101 (5)(Pt. 1), 2603–2614.

Thorne, P.D., Taylor, J., 2000. Acoustic measurements of boundary layer flow and sediment flux. Journal of the Acoustical Society of America 108 (4), 1568–1581.

Thorne, P.D., Butler, M.B., 2001. Measurements of the scattering properties of suspensions of marine sand. Conference held at the Southampton Oceanographic Centre 9-12 April 2001. Acoustical Oceanography 23 (2), 392–398.

Thorne, P.D., Hayhurst, L., Humphery, V.F., 1992. Scattering by non-metallic spheres. Ultrasonics 30, 15–20.

Thorne, P.D., Hardcastle, P.J., Soulsby, R.L., 1993. Analysis of acoustic measurements of suspended sediments. Journal of Geophysical Research 98 (C1), 899–910.

Thorne, P.D., Waters, K.R., Brudner, T.J., 1995a. Acoustic measurements of scattering by objects of irregular shape. Journal of the Acoustical Society of America 97 (1), 242–251.

Thorne, P.D., Holdaway, G.P., Hardcastle, P.J., 1995b. Constraining acoustic backscatter estimates of suspended sediment concentration profiles using the bed echo. Journal of the Acoustical Society of America 98 (4), 2280–2288.

Thorne, P.D., Sun, S., Zhang, J., Bjorno, I., Mazoyer, T., 1997. Measurements and analysis of acoustic backscattering by elastic cubes and irregular polyhedra. Journal of the Acoustical Society of America 102 (5)(Pt. 1), 2705–2713.

Thorne, P.D., Hardcastle, P.J., Bell, P.S., 1998a. Application of acoustics for measuring nearbed sediment processes: an integrated approach. Oceans '98 Conference Proceedings, 28 September–1 October, Vol. 1, Nice, pp. 438–441.

Thorne, P.D., Hardcastle, P.J., Dolby, J.W., 1998b. Investigation into the application of cross-correlation analysis on acoustic backscattered signals from suspended sediment to measure nearbed current profile. Continental Shelf Research 18 (6), 695–714.

Thosteson, E.D., Hanes, D.M., 1998. A Simplified method for determining sediment size and concentration from multiple frequency acoustic backscatter measurements. Journal of the Acoustical Society of America 104 (2)(Pt. 1), 820–830.

Traykovski, P., Hay, A.E., Irish, J.D., Lynch, J.F., 1999. Geometry, migration, and evolution of wave orbital ripples at LEO-15. Journal of Geophysical Research 104 (C1), 1505–1524.

van Unen, R.F., Thorne, P.D., Cox, J., Kamminga, S.D., 1998. Laboratory measurements of current flow using cross-correlation on acoustic scattering from suspended sediments. Journal of the Acoustical Society of America 104 (3), 1345–1355.

Vincent, C.E., Green, M.O., 1990. Field measurements of the suspended sand concentration profiles and fluxes and of the resuspension coefficient γ_0 over a rippled bed. Journal of Geophysical Research 95 (C7), 11 591–11 601.

Vincent, C.E., Osborne, P.D., 1993. Bedform dimensions and migration rates under shoaling and breaking waves. Continental Shelf Research 13 (11), 1267–1280.

Vincent, C.E., Hanes, D.M., Bowen, A.J., 1991. Acoustic measurements of suspended sand on the shoreface and the control of concentration by bed roughness. Marine Geology 96, 1–18.

Vincent, C.E., Marsh, S.W., Webb, M.P., Osborne, P.D., 1999. Spatial and temporal structures of suspension and transport over megaripples on the shore face. Journal of Geophysical Research 104 (C5), 11 215–11 224.

Vincent, C.E., Hanes, D.M., Dohmen-Janssen, C.M., Klopman, G., McLean, S.R. Ribberink, J.S., 2001. Suspension by regular and group waves over bedforms in a large wave flume (SISTEX 99). In: H. Hanson, M. Larson (Eds.), Proceedings of Coastal Dynamics'01, Lund, Sweden, pp. 303–312.

Voulgaris, G., Trowbridge, J.H., 1998. Evaluation of the acoustic Doppler velocimeter (ADV) for turbulence measurements. Journal of Atmospheric and Oceanic Technology Vol. 15, 272–289.

Weltner, K., Grosjean, J., Schuster, P.,Weber, W.J., 1986.Mathematics for Engineers and Scientists. Stanley Thomes Ltd, UK, pp. 512 (Chapter 10).

Williams, J.J., Rose, C.P., Thorne, P.D., O'Connor, B.A., Humphery, J.D., Hardcastle, P.J., Moores, S.P., Cooke, J.A., Wilson, D.J., 1999. Field observations and predictions of bed shear stresses and vertical suspended sediment concentration profiles in wave-current conditions. Continental Shelf Research 19, 507–536.

Williams, J.J., Bell, P.S., Thorne, P.D., Trouw, K., Hardcastle, P.J., Humphery, J.D., 2000. Observed and predicted vertical suspended sediment concentration profiles and bedforms in oscillatory-only flow. Journal of Coastal Research 16 (3), 698–708.

Wilson, R.A., Thorne, P.D., Williams, J.J., Bell, P.Hardcastle, P.J., 2000. An evaluation of a 3D acoustic coherent Doppler current profiler in the marine environment. In: Manell E. Zakhatia (Eds.), Proceedings of the Fifth European Conference on Underwater Acoustics ECUA 2000, Vol. 1, 10–13 July 2000, Lyon, France. EU, Luxembourg, pp. 627–632.

Young, R.A., Merrill, J.T., Clarke, T.L., Proni, J.R., 1982. Acoustic profiling of suspended sediments in the marine bottom boundary layer. Geophysical Research Letters 9, 175–178.

Zedel, L., Hay, A.E., Cabrera, R., Lohrmann, A., 1996. Performance of a single-beam pulse-to-pulse coherent Doppler profiler. IEEE Journal of Oceanic Engineering 21, 290–297.

Zedel, L., Hay, A.E., 1999. A coherent Doppler profiler for high resolution particle velocimetry in the ocean: laboratory measurements of turbulence and particle flux. Journal of Atmosphere and Ocean Technology 16, 1102–1117.

Zedel, L., Hay, A.E. A Three component bistatic coherent Doppler velocity profiler: Error sensitivity and system accuracy. IEEE Journal of Oceanic Engineering, personal communication, submitted for publication.